

# Accepted Manuscript

Review

Friction stir welding/processing of polymers and polymer matrix composites

Yongxian Huang, Xiangchen Meng, Yuming Xie, Long Wan, Zongliang Lv,  
Jian Cao, Jicai Feng

PII: S1359-835X(17)30439-6

DOI: <https://doi.org/10.1016/j.compositesa.2017.12.005>

Reference: JCOMA 4854

To appear in: *Composites: Part A*

Received Date: 12 September 2017

Revised Date: 22 November 2017

Accepted Date: 4 December 2017



Please cite this article as: Huang, Y., Meng, X., Xie, Y., Wan, L., Lv, Z., Cao, J., Feng, J., Friction stir welding/processing of polymers and polymer matrix composites, *Composites: Part A* (2017), doi: <https://doi.org/10.1016/j.compositesa.2017.12.005>

This is a PDF file of an unedited manuscript that has been accepted for publication. As a service to our customers we are providing this early version of the manuscript. The manuscript will undergo copyediting, typesetting, and review of the resulting proof before it is published in its final form. Please note that during the production process errors may be discovered which could affect the content, and all legal disclaimers that apply to the journal pertain.

**Friction stir welding/processing of polymers and polymer matrix composites**

Yongxian Huang\*, Xiangchen Meng, Yuming Xie, Long Wan, Zongliang Lv, Jian  
Cao, Jicai Feng

State Key Laboratory of Advanced Welding and Joining, Harbin Institute of  
Technology, Harbin 150001, China

\*Corresponding author: Email: [yxhuang@hit.edu.cn](mailto:yxhuang@hit.edu.cn) (Tel. +86-451-86413951; Fax  
+86-451-86416186)

**Abstract:** Friction stir welding/processing (FSW/P) involving temperature, mechanics, metallurgy and interaction, is a complex solid state joining and processing technology. FSW has been widely applied to join aluminum alloy, titanium alloy and other materials which are difficult to weld by fusion welding. The last scientific study states that FSW has potential to join thermoplastic polymers and polymer matrix composites. In this review, current understanding and development about FSW of thermoplastic polymers and polymer matrix composites, multifunctional composites fabrication as well as dissimilar FSW of metal and polymer are reviewed. Future scientific research and engineering development related to FSW/P of thermoplastic polymers and polymer matrix composites are identified.

**Keywords:** Polymers/polymer matrix composites; Friction stir welding/processing; Mechanical property; Thermo-mechanical behavior.

## Catalogue

<b>Abstract:</b> .....	<b>1</b>
<b>0 Introduction</b> .....	<b>2</b>
<b>1 Friction stir welding process of polymers</b> .....	<b>4</b>
1.1 Welding Process .....	4
1.1.1 Equipment parameters .....	5
1.1.2 Welding tool .....	7
1.2 Thermo-mechanical behavior .....	9
1.3 Mechanical properties .....	10
1.4 Welding defects .....	12
1.5 New methods eliminating defects .....	14
1.5.1 Stationary shoe friction stir welding .....	15
1.5.2 Double-pass and self-reacting friction stir welding .....	18
1.5.3 Submerged and additive friction stir welding .....	19
1.6 Brief summary .....	20
<b>2 Preparation of multifunctional polymer matrix composites</b> .....	<b>20</b>
2.1 In-situ friction stir processing .....	21
2.2 Stationary shoe friction stir processing .....	21
2.3 Submerged friction stir processing .....	23
2.4 Brief summary .....	23
<b>3 Dissimilar friction stir welding of polymer and metal</b> .....	<b>23</b>
3.1 Mechanical interlocking .....	24
3.2 Effect of surface pre-treatment on adhesive mechanism .....	26
3.2.1 Mechanical and chemical pre-treatments .....	26
3.2.2 Electrochemical pre-treatment .....	27
3.3 Limitation for friction stir welding of metal and polymer .....	29
3.4 New technique of friction spot joining for polymer and metal .....	29
3.4.1 Principles of friction spot joining .....	29
3.4.2 Process development of friction spot joining .....	30
3.5 Brief summary .....	32
<b>4 Conclusion and future outlook</b> .....	<b>32</b>
<b>Acknowledgements</b> .....	<b>34</b>
<b>References</b> .....	<b>35</b>

## 0 Introduction

Basing on the advantages of high specific strength, good corrosion resistance, excellent design freedom and processing ability, polymers and polymer matrix composites have the potential to reduce costs and improve production efficiency with low environmental impact in aerospace, automobile and electronic devices [1, 2]. However, the fabrication of larger and complex parts usually requires joining

technology, such as adhesive bonding, mechanical fastening and welding techniques [3]. Generally, mechanical fastening is easy to manipulate, stress concentration easily appears at the bonding region decreasing joint reliability, while joining part results in the increase of weight deteriorating the design of lightweight. Adhesive bonding is relatively mature. However, adhesive bonding needs long process cycle. Meanwhile, impact resistance, fatigue resistance and humidity resistance are insufficient, reducing joint property.

Up to now, the most efficient joining method is welding process, such as electric resistance welding, ultrasonic welding, hot plate welding, linear vibration welding, friction stir welding (FSW) and so on [3]. These welding methods mainly consist of three processes: (a) formation of a layer of molten material on the surfaces to be joined, (b) bonding formation by upsetting and (c) the molten material cools, and the stage pressure should be maintained to prevent voids forming inside the weld zone [4]. Table 1 shows comparison of process requirements for different welding methods [1]. Ultrasonic welding mainly performs spot welding, while machines and tools are expensive, and part preparation is time consuming. For hot gas and extrusion welding techniques, a v-groove is required for proper joint formation at a very slow rate, and the properties are highly dependent on the operator's skill level. Friction welding needs flatten face and the machine costs are relatively high.

FSW owns the advantages of no preparation, low process time and machine/tool consumable costs as well as low temperature, severe plastic deformation and high joint quality, which has potential to overcome the deficiency in above-mentioned welding methods [5]. Schematic diagram of FSW process is shown in Fig. 1. During FSW, a rotational tool owning a special-designed shoulder and a pin, frictions with the workpieces to weld at a high rotational velocity, producing frictional heat to soften the materials and generating material flow to mix and join the welded materials. However, different from metal, FSW of thermoplastic polymers is not a solid state process because polymers consist of molecules with different chain lengths and the polymers do not have definite melting point, but rather melting ranges [6]. When applying FSW/P to polymers, some shorter chains may reach their melting point, while longer

chains are still solid state. FSW is firstly applied in thermoplastic polymers in 1997 [1]. However, seldom works have been reported due to its immature then. Until 1999, Clark et al. [7] developed different types of tools to join thermoplastic polymers. The real research on FSW of thermoplastic polymers begins gradually. The systematical research starts in 2005, especially after 2009 [8]. Up to now, FSW has successfully realized the joining of thermoplastic polymers and polymer matrix composites, such as various grades of Poly Ethylene (PE) [9], Poly Propylene (PP) [10], Poly Carbonate (PC) [11], Acrylonitrile Butadiene Styrene (ABS) [12], Polymethyl Methacrylate (PMMA) [13], Poly Caprolactam (Nylon 6) [14], Poly Ethylene Terephthalate (PET) [15], 30% glasses fiber-reinforced PP composite [16] and 20% carbon fiber-reinforced PP composite [17], and obtained some satisfactory results.

Nowadays, FSW has become one of the most important welding technologies for thermoplastic polymers. In this paper, the aspects of FSW of thermoplastic polymers and polymer matrix composites (welding process variables, mechanical properties, thermo-mechanical behavior and new technologies of FSW for eliminating defects), fabrication of multifunctional composites as well as dissimilar FSW of metal and polymer are reviewed. Meanwhile, the scientific study and engineering application in the future are pointed out on these basics.

## **1 Friction stir welding process of polymers**

### **1.1 Welding Process**

During FSW of thermoplastic polymers and polymer matrix composites, the key factors influencing joint formation and quality can be separated into three categories: equipment parameters, welding tool parameters and material properties [18]. The processing variables of FSW are shown in Fig. 2.

Welding tool and equipment parameters are mainly dependent on mechanical properties of polymers, such as yield strength, ductility and hardness, which play significant influences on plastic deformation [19]. High heat input is required for a high melting point or constant-pressure specific heat material, while the materials with a low melting point or constant-pressure specific heat need relative lower heat input [20]. Thermal properties of material primarily affect welding peak temperature

and thermal transfer. For the materials with a high thermal conductivity which easily results in the amounts of heat loss, high heat input is necessary to guarantee sufficient heat input, obtaining sound joint [21]. Oppositely, thermal conductivity of polymer is lower than Al alloys, which is difficult to transfer heat to preheat the materials at the front of the rotational tool. Therefore, higher heat input is also required to attain sound joint.

### 1.1.1 Equipment parameters

Rotational velocity ( $\omega$ ) and welding speed ( $v$ ) control the amount of heat input during FSW, which in turn affect the crystallinity and resultant properties. The lower the heat input, the smaller the crystallinity, and vice-versa, under the premise of sufficient heat input to soften materials. High rotational velocity provides large amounts of heat input, while low welding speed increases the duration of high temperature exposure, and vice-versa. In addition, plunging depth and tilting angle are closely correlated with contacting area and overflowing of plasticized materials between shoulder and workpieces, which affect joint quality of polymer. Most researchers investigate the works about influences of welding process parameters on joint formation and quality by reviewing published literatures, and the optimum combination of rotational velocity and welding speed has been concluded, as shown in Table 2. Aydin et al. [22] studied effect of welding parameters on joint formation based on a screwed pin. Increasing rotational velocity excessively increased surface heat input, resulting in coarse joint surface. Zafar et al. [14] employed a screwed pin to join 9 mm thick Nylon 6 sheet. Low rotational velocity could improve joint formation, while high rotational velocity and big tilting angle easily increased peak temperature, leading to the bubbles and overflowing of molten or plasticized materials. Buzkurt et al. [23] employed a conventional tool containing a shoulder of 18 mm diameter and a pin of 6 mm diameter to join PE sheet and showed that welding temperature varied at the range of 120~165 °C under a high rotational velocity, which exceeded the melting point of the PE polymer, resulting in the pores and cavity defects and then deteriorating joint formation. They also expounded that the rotational

velocity played an important role and contributed 73.85% of the overall welding parameters. The tilting angle exerted the least effect in comparison with other welding parameters. Mendes et al. [24, 25] observed that rotational velocity and axial force values above a certain threshold were required to provide defect-free joint. Jaiganesh et al. [26] expounded that low welding speed was essential to obtain better joining of PP. High rotational velocity resulted in overheating and melting of materials and then came out as the tool rotated. At a welding speed of 10 mm/min, a rotational velocity of 1000 rpm and a tilting angle of  $1^\circ$ , the optimum joint was attained. Hoseinlghab et al. [27] found that quality and creep resistant of joint decreased with increasing tilting angle. A tool without tilting angle was recommended. Payganeh et al. [16] stated that tensile strength of joint increased when tilting angle varied from  $0\sim 2^\circ$ . Tilting angle affected the vertical and horizontal material flows. Improper tilting angle could cause tunnel and crack-like defect in the joint. At the tilting angle of 0, insufficient vertical and horizontal material flows may lead to defects, reducing tensile strength. Increasing tilting angle improved material flow characteristics, and hence tool movement forged welding material better to fill the defect, increasing joint strength. Payganeh et al. [16] performed FSW of PP matrix composites with 30% glasses fiber and found that low joint strength was attributed to tunnel defect. The formation of the tunnel defect is caused by excessive turbulence at a high rotational velocity.

Sadeghian et al. [12] found that tilting angle and diameters ratio in high-levels as well as rotational velocity in low-level were optimum conditions during FSW of ABS sheet. In addition, welding speed in a high-level has significant detrimental effect on joint strength. Under a tilting angle of  $2^\circ$ , a rotational velocity of 900 rpm, a rotational tool with shoulder/pin diameters ratio equaling to 20/6 and a welding speed of 25 mm/min, welding joint equivalent to the yield strength of parent ABS sheet was achieved. Mostafapour et al. [4] also studied effect of plunge depth on FSW joint formation of PE sheet with the thickness of 9 mm. Low plunge depth (lower than 0.5 mm) resulted in coarse surface, while big plunge depth resulted in big flashes and stress concentration, decreasing mechanical property.

### 1.1.2 Welding tool

As an important part of FSW equipment, welding tool owning different topology characteristics is the core for high quality FSW joint. Geometry features of welding tool mainly consist of shoulder and pin diameters, shoulder and pin features, pin shape and pin length [5, 6]. Frictional heat, thermo-mechanical behavior and resultant macro/micro-structure are influenced by geometry features of welding tool as same as equipment variables. During conventional FSW of Al alloys, the shoulder is responsible for large amounts of heat generation, which occupies about seventy-five percent of the total heat input and the resultant heat input is generated by pin and plastic deformation [28]. Large shoulder diameter results in high heat input and then improves material flow, obtaining sound joint, while small shoulder diameter leads to insufficient frictional heat and material flow, causing defect at the nugget zone (NZ). However, because of low thermal conductivity of polymer, frictional heat produced by the shoulder is mainly concentrated on the surface of joint, which is difficult to transfer through the thickness direction [13]. Therefore, rotational pin is the primary responsibility for frictional heat and material flow during FSW of polymer to obtain high quality joint. Some critical issues related to FSW tools of polymer especially the geometry features of pin are briefly discussed. Welding tools used in the published papers during conventional FSW of polymer are listed in Table 3.

Panneerselvam et al. [29, 30] investigated effect of pin geometry on the tool force and joint defect during FSW of PP. A taper and a straight pin profiles produced more linear force, which was insufficient to soften materials, while a threaded pin profile could produce less amount of force. The triangular, square or groove with square pin profile could produce sound joint. Panneerselvam et al. [31] also reported that a smooth taper pin was detrimental to joint formation under all chosen welding parameters, while the joint with good formation and high quality was achieved using a taper screwed pin. Moreover, Panneerselvam et al. [32] investigated effect of rotational direction of a screwed pin on material flow and joint formation during FSW of Nylon 6 polymer. For the clockwise rotation, a left screwed pin provided the



channel for overflowing of plasticized materials, leading to big flashes and cavity defects. When using a right screwed pin, the rotation of pin could drive plenty of plasticized materials flow from the bottom to the tip of pin, reducing flashes and avoiding welding defect.

Besides, Jaiganesh et al. [26] studied effect of tool profiles (square, cylindrical and triangular threaded pins) on tensile strength and found that the best joint was given using a triangular threaded pin. Padmanaban et al. [33] stated that a screwed pin generated more heat input, improving material flow in the NZ. Additionally, the screwed pin exerted an extra downward force, which was beneficial to accelerate plasticized material flow and then attain sound joint. Moreover, Payganeh et al. [16] discussed effect of a taper pin with groove, a triangle pin with screw thread, a triangle pin and a cylindrical pin with groove on joint formation of 30% glass fiber-reinforced PP polymer. The triangle pin with screw thread owned sufficient contacting area with workpieces to be welded, which generated bigger frictional heat and sufficient material mixture, achieving good joint formation. The other three welding tools had lower contacting area with workpieces to be welded, deteriorating material flow and joint formation. According to the result of Elangovan et al. [34], a square pin produced more pulse/sec compared with a pin without squares. The square pin produced 80 pulses per second ( $\text{pulses/s} = \text{rotational velocity in second} \times \text{number of flat faces}$ ) and a triangular pin profile provided 60 pulses per second at a rotational velocity of 1200 rpm, while no such pulsating action was observed in a cylindrical, tapered or threaded pin. Therefore, a triangle pin with screwed thread may be more suitable for FSW of polymer. Additionally, Kiss and Czigány [35] demonstrated that a denser groove distribution on the pin presented better results. Hoseinlghab et al. [27] showed that a pin with cylindrical geometry was preferred in comparison to a pin with conical geometry at the same parameters. Pin geometry is relatively independent of welding parameters. Sadeghian et al. [12] stated that the highest strength efficiencies of welded joints were equivalent to 101% of base material (BM) by a conical pin (a rotational velocity of 900 rpm, a welding speed of 25 mm/min and a tilting angle of  $2^\circ$ ) and 99% of BM by a cylindrical pin (a rotational velocity of 1400 rpm, a welding

speed of 16 mm/min and a tilting angle of  $1^\circ$ ), respectively. These results may be dependent on different welding process windows.

Except the above-mentioned welding process variables, an additional preheating temperature plays a vital role on FSW of polymer with low thermal conductivity and macromolecular. Adyin et al. [22] adopt three preheating modes containing room temperature, backing preheating temperatures of  $50^\circ\text{C}$  and  $80^\circ\text{C}$  to join 4 mm thick ultra high molecular weight PE (UHMW-PE) sheet. Welding pre-heating promoted joint formation and then realized the welding at a low rotational velocity. Meanwhile, the maximum tensile strength obtained at the  $50^\circ\text{C}$  was about 124% of that at the room temperature due to homogeneous temperature distribution along the thickness direction induced by backing pre-heating. Moreover, Vijendra et al. [36] developed an induction-heated tool assisted FSW to weld 5 mm thick high density PE (HDPE) sheet, in which an induction coil encircled the welding tool. Induction heating of tool enabled materials to be plasticized in a short time and to be easily stirred. The optimum conditions for the maximum joint strength were a tool-pin temperature of  $45^\circ\text{C}$ , a welding speed of 50 mm/min and a rotational velocity of 2000 rpm. It is postulated that pre-heating on the crystallization mechanism attributes to the improvement of tensile strength, which merits further investigation in future studies.

## 1.2 Thermo-mechanical behavior

Thermo-mechanical behavior is the key factor affecting joint formation and mechanical property, which is mainly controlled by welding tool variables and material properties. Simões et al. [13] expounded thermo-mechanical and material flow behaviors during FSW of PMMA polymer in details, and stated the differences between polymer and metal. The results showed that the interface between BM and NZ at the advancing side (AS) was opaque indicating small discontinuous phenomenon, while the interface between BM and NZ at the retreating side (RS) exhibited opaque weak joining completely. Because of low thermal conductivity and mechanical properties of polymer, the deformed zone and material flow behavior of polymer had some special characteristics (Fig. 3), as followed: (1) small deformed zone, and no obvious shoulder affected zone (region III) and pin tip affected zone (IV);

(2) rotational pin played a key influence on joint formation and the shoulder could be neglected; (3) molten or plasticized materials easily overflowed out from the two sides of shoulder, but not into NZ, resulting in the loss of region III; (4) morphology of pin affected zone kept straight and parallel to the shape of rotational pin, leading to small thermo-mechanically affected zone (TMAZ) and the loss of region IV, which was the main reason for lack of root penetration; (5) molten or plasticized materials easily overflowed and then caused the discontinuous interface, while welding temperature of RS was lower than of AS, which was the other reason for discontinuous interface of RS.

Zafar et al. [14] employed tracing method (red ABS owning better tracer) and a right screw pin to investigate material flow behavior using 16 mm thick Nylon 6 sheet (Fig. 4). Along the X-axis perpendicular to the welding direction, plasticized materials at the AS and RS all diffused and well distributed at the NZ. Meanwhile, insufficient mixing material close to the top of joint was induced by without screw on the bottom of pin. Along the Y-axis parallel to the welding direction, rotation of pin caused that plasticized material could be driven into the back of pin and the bigger driven distance of 11 mm resulting from squeezing effect (Fig. 4d). Along the Z-axis through the thickness direction, the tracing material on the bottom was upward into the top under the rotation and squeezing effects of pin. For the tracing materials on the middle, the same phenomenon as same as the bottom was found, while the marked material on the top slightly downward to the bottom and plenty of materials overflowed out of the NZ, producing big flashes. However, there is no obvious differences between AS and RS (Fig. 4e).

### 1.3 Mechanical properties

Mechanical properties of FSW joint of polymer are closely linked with crystallinity and inside welding defects such as weak bonding, micro-crack, bubbles, lack of root penetration and so on. Insufficient frictional heat leads to inadequate material flow or higher heat input results in the overflowing out of plasticized materials, which causes the formation of defect and then becomes the initiation of crack, reducing tensile property. Moreover, lower heat input or faster cooling rates

reduces crystallinity, decreasing hardness and ability of load bearing. Saeedy et al. [9] employed FSW to join PE and found that tensile strength reached 75% of BM under a rotational velocity of 1400 rpm, a welding speed of 12 mm/min and a tilting angle of 1°. Squeo et al. [37] expounded that yield strength was comparative with BM of PE under a welding speed of 28 mm and a rotational velocity of 6000 rpm, while fracture mode presented brittle fracture. In addition, Aydin et al. [22] used backing preheating to perform FSW of PE sheet with the thickness of 4 mm. Under a welding speed of 10 mm/min, a rotational velocity of 960 rpm and a preheating temperature of 50 °C, tensile strength was equivalent to 89% of BM, which was higher than 72% without preheating joint, but the elongation still indicated lower value. In order to increase efficiency, reduce experimental cost and quickly search optimum parameters, most researchers employ orthogonal experimental method to perform optimum experiment. Ahmadi et al. [17, 38] stated that welding speed had biggest influences on shear strength and the influence of tilting angle was smallest during FSW of 20% carbon fiber-reinforced composites. The contributions of welding speed, rotational velocity and tilting angle are 79.1%, 12.3% and 5.4%, respectively. Kiss and Czigany [35] found out that the strength of NZ was less than 50% during FSW of PP, which resulted from non-uniform crystallization rate of material.

Having reviewed the published literatures, the applications of FSW on thermoplastic polymers have been investigated, but a high quality joint is difficult to achieve. Maximum tensile strengths of all FSW joints are obtained in the experimentations, as listed in Fig. 5. Tensile property of joint is relatively lower than BM. However, all FSW joints of PP are far higher than those by other welding methods (Fig. 6), which indicates FSW is an efficient method to join polymers. Moreover, one noteworthy property has not been reported in these literatures is the elongation of joint. It has been noted that tensile strength could be quite high, while the elongation at failure was very low and presented brittle fracture. Whereas the BM may reach elongation of 100~150%, a welding joint only attains 10~15% or even less. The reason for dramatic difference is unknown, perhaps due to the low ductility of polymer and micro crack on the RS. Meanwhile, welding residual stress is also the

main reason of micro crack, deteriorating tensile property. Simões et al. [13] found that residual stress could result in the occurrence of crack by observing the specimen one month after FSW, which was detrimental to fatigue performance.

Microhardness, an important evaluating index of mechanical property, reacts the ability resisting to local deformation of material, which is affected by crystallinity. It is observed that the hardness of PE polymer matrix changes from 92 RH to 95 HR, while the hardness at NZ of joint is lower than BM, ranging from 65 HR to 85 HR [31]. The reason is the low crystallinity induced by big cooling rates. The hardness on the AS is higher than that on the RS resulting from high frictional heat on the AS. In fact, an uneven distribution during FSW results in the differences of crystallinity at different regions, affecting hardness. In order to analyze the crystallinity, Gao et al. [39] performed differential scanning calorimetry (DSC) for different regions of PE joint to analyze the crystallization behavior induced by uneven temperature distribution. According to formula,

$$W_c = \frac{\Delta H_m}{\Delta H_m^0} \times 100\% \quad (1)$$

where  $\Delta H_m$  was the melting enthalpy of the sample, and the  $\Delta H_m^0$  was the melting enthalpy of perfectly crystalline PE, of which the value was 293 J/g. The crystalline contents of different conditions of BM, heat affected zone (HAZ), TMAZ, and NZ were 54.5%, 54.0%, 51.1% and 48.2%, respectively (Fig. 7). There is no obvious HAZ due to low thermal conductivity. However, the crystalline of TMAZ and NZ significantly reduced due to low cooling rates induced by high welding speed. The decrease of crystalline attributed to the reduction in the density, hardness and tensile property. Vijendra et al. [36] also stated that pre-heating could lessen the reduction in hardness. Therefore, from the viewpoint of improving mechanical property, the research aiming at enhancing crystallinity of FSW joint of polymer is extremely necessary, in which pre-heating or nucleating agents may be worth considering.

#### 1.4 Welding defects

FSW has acquired some results at the joining of polymers, but the relevant

research project is still in the feasibility. Under improper welding process parameter or welding tool, welding defects unavoidably appear at the FSW joint of polymer, deteriorating joint formation and mechanical property. Table 4 exhibits common defects at the joint during FSW of polymer, such as flashes, surface lack of filling, lack of root penetration, blowhole, voids at the RS and tunnel.

During FSW of polymer, insufficient material flow induced by low frictional heat easily leads to cavity or tunnel defect in the NZ, which is controlled by plunging depth, rotational velocity and welding speed. Generally, the two defects always form at the AS. For the materials at the AS of joint, shearing force and pressure force are in the opposite directions, while the directions of these two forces at the RS are identical. Therefore, more materials flow into the RS of joint behind the rotational pin, which makes the cavity or tunnel defect appear at the AS of joint. Surface lack of filling is the worst case of cavity or tunnel defect due to the extreme inadequate material flow [17]. Aiming at the phenomenon of thickness reduction, Zafar et al. [14] explained that high rotational velocity resulted in that overheat materials and semi-molten Nylon 6 were squeezed out of NZ, which decreased the thickness of NZ, reducing tensile strength.

Pores are commonly associated with the evolution of structural water, entrapment of air, products of thermal degradation or differential thermal expansion along the affected volume [40, 41]. Abibe et al. [40] expounded that when PEI was not dried prior to joining and contained about 0.48% structural water in weight, structural water may have vaporized and constituted part of the pores. Tan et al. [41] proposed a hypotheses of thermal degradation and differential thermal expansion during laser-joined carbon fiber reinforced polymer/steel joint. Porosities originating from differential thermal expansion presented irregular rough inner walls, whereas evolution of gaseous products from thermal degradation created pores with smooth inner walls. The occurrence of pores always reduces the area of load bearing, and then becomes crack source, decreasing mechanical property.

Void at the RS is a fatal defect, which always appears at the polymer joint. It tends to become the source of stress concentration and then results in joint fracture.

During FSW, the materials in the AS undergo larger plastic deformation than those in the RS, which make that the heat of plastic deformation in the AS is more than that in the RS. Therefore, the temperature of materials at the AS is higher than that at the RS. The poor thermal conductivity of polymer restricts heat conduction from the AS to the RS. Therefore, due to lack of sufficient heat at the RS, the materials are not stirred properly into the NZ at the RS of joint. Consequently, the voids defect occurs at the RS. Besides the voids at the RS, another important defect is lack of root penetration. For FSW of alloys with high thermal conductivity, the lack of root penetration is closely correlated with shorter pin length, smaller plunge depth and so on. However, polymers possess low thermal conductivity (lower than  $0.5 \text{ Wm}^{-1}\text{K}^{-1}$ ), the materials between the surface of pin tip and backing plate are difficult to be heated and softened. Under low peak temperature, these materials can not be stirred and flow, resulting in the lack of root penetration. This defect always decreases the area of load bearing and becomes the crack source, reducing tensile property. Arici et al. [42] performed single pass FSW of 3 mm thick medium density PE (MDPE) sheet and expounded that the thickness of root defect was approximately equivalent to the difference between the sample thickness and the pin length ( $\approx 0.2 \text{ mm}$ ), which validated that the materials near the bottom were not affected by rotational pin [13]. Moreover, the joint was easily bended into two parts with a small force even by hand, reducing tensile properties heavily.

### **1.5 New methods eliminating defects**

According to the above-mentioned, during conventional FSW of polymers and polymer matrix composites, when welding parameter or welding tool is not reasonable, the problems of bad surface formation, lack of root penetration and low crystallinity are detrimental to joint formation and property. Therefore, in order to enhance material flow, thermal conductivity or cooling rates during FSW and then improve joint formation, researchers have attempted stationary shoe FSW, submerged FSW and additive FSW (adding third materials). In this review, the new techniques are classified by characteristics of welding defects, while the detailed contexts are as followed.



### 1.5.1 Stationary shoe friction stir welding

Because of low viscosity and thermal conductivity, the main difficulty for FSW of polymers is the lack of frictional heat generated through contact between rotational tool and BM. Therefore, a stationary shoe tool was invented by Strand [1] consisting of a rotational pin, a stationary shoe and a heater, which exhibited the huge potential advantages to join polymers. The main role of the pin was to produce frictional heat for softening and stirring materials within the joint. The stationary shoe was utilized to contain the displaced materials and hold it on the NZ, while it cooled. The heater, equipped with a closed-loop thermo-controller, was responsible for supplying additional heating to the workpieces and slowing down the cooling rates of materials. Up to present, microstructure, mechanical property and optimization of process parameters during stationary shoe FSW have been widely studied. Strand [1] firstly stated that the macrostructure of joint was divided into three regions, which were BM, interface transition zone and NZ, as indicated in Fig. 8. Onion ring appeared at the NZ, which resulted from the overlap of plasticized materials softening layer, while there was no obvious HAZ. Moreover, lack of root penetration defect occurred at the bottom, becoming crack initiation.

Based on the tooling system designed by Strand [1], Mostafapour et al. [43, 44] designed a welding system, in which a heater was located at the back of a pin, as exhibited in Fig. 9. Results showed that dwell times of least 10~15 s starting the process were necessary, which created a pool of semi-molten polymer and expanded the zone of softened materials. When the molten materials were developed, the materials tended to stick to the shoe, which resulted in residual stress concentration on the top of joint, leading to considerable reduction of tensile strength. The material adhesion was avoided by coating the tool shoe with Poly Tetra Fluoro Ethylene (PTFE). High rotational velocity and shoulder temperature extended NZ, which resulted in good combination of molecular chains and reduction of incomplete root penetration, achieving high joint performance. Mostafapour et al. [4] also employed the above-mentioned tool to join Nylon 6 successfully. Utilizing heat assisted FSW,



the reduction of cooling rates could lead to an increase in crystallinity of joint and then improved mechanical property. Ultimate tensile strength over 98% of BM was attained under optimum process parameters. Table 5 lists the optimum combination of process parameters for stationary shoe FSW of polymers.

Based on experimental and analyzed results, Azarsa et al. [45] performed stationary shoe FSW of HDPE and stated that the combination of high rotational velocity and low welding speed increased flexural strength by reducing size of defects. Mendes et al. [46] presented a novel FSW robotic platform for welding polymers, as displayed in Fig. 10. It was feasible to join ABS in high quality using robotic FSW platform aided by force/motion control, which was also applied to join other polymers by changing loads capacity, welding tool and parameters. High axial force promoted the squeeze of the molten materials, which helped cooling of the joint and then avoided shrinkage and voids. Meanwhile, sound joint presented the same hardness as BM. Mendes et al. [15] performed FSW of 6 mm thick ABS sheet using stationary shoe without heating system, which validated that it was feasible to produce high quality joint. The axial force contributed to material mixing and prevented the formation of cavities at the RS of NZ. High strength efficiency was achieved only when a high rotational velocity and a high axial force were used.

Rahbarpour et al. [47] performed FSW of wood/polymer composites by a stationary shoe with heating system to eliminate the problems of voids and poor mixing. Maximum tensile strength of the welded wood-polymer composites was 92.95% of BM, at a condition of medium rotational velocity, low temperature and high welding speed. Rezgui et al. [48] used a stationary shoe made of wood to weld HDPE and identified models were used to simulate by finite element. Better coherences between numerical predictions and experimental observations in different cases of mechanical behavior were achieved. Eslami et al. [49] stated that one of the main challenge during stationary shoe FSW was to prevent the overflowing of the soften materials inside the shoulder and then caused shoulder fail, especially during long joint. In order to avoid the problem, different materials sleeves (PC, teflon, aluminum, wood and brass) and rotational shoulders owning different diameters have

been developed and analyzed. Based on the deficiencies of aluminum, brass and wood shoulders, a teflon polymeric stationary shoe was designed and proved to be the best option, resulting in superior surface quality, as shown in Fig. 11. The reason was that an outer sleeve made of copper gave an additional degree of freedom for a brass sleeve as well as absorbing heat. Moreover, the applied force was kept constant using stationary shoe, while the same behavior could not be found using a rotational shoulder. Eslami et al. [50] employed the above-mentioned optimum welding tool to join dissimilar PP/PE polymers. At a low welding speed, material degradation possibly occurred due to excessive heat generation. It was proven to be a good advantage for metal applications. Hajideh et al. [51] carried out dissimilar joining of PE/PP polymers using stationary shoe FSW, while four different tool pins (threaded cylindrical, squared, triangular and straight cylindrical) were employed. Utilizing the threaded cylindrical pin provided more uniform material flow than other pins. In optimum condition, sound joint with uniform microstructure, strength equal to 98% of PE, high elongation and hardness than PE was achieved.

In additional, Kiss and Czigány [52] demonstrated that a denser groove distribution in pin collected the material behind the tool instead of accumulating it, and gave better results under identical welding conditions compared with a tool with lower groove slope. The mechanical properties of joint were related to the K factor ( $K = (\text{rotational velocity/welding speed}) \times \text{tool diameter}$ ), a proper quality joint could be produced in the 150~400 range. A bending type stress arose in the joint, which were compression on the crown side and tension on the root side. They also [15] successfully employed a stationary shoe without heating system to join amorphous Poly Ethylene Terephthalate-co-1,4-cyclohexylenedimethylene Terephthalate (PETG) which was difficult to be welded using a conventional tool. Stirring action of rotational pin could break spherulite and make them random distributed, as shown in Fig. 12. The spherulite size of BM ranged from 10  $\mu\text{m}$  to 25  $\mu\text{m}$ , while the spherulite size of NZ had smaller size with 10~20  $\mu\text{m}$ . Meanwhile, the author also deeply studied the microstructures of transition zone, indicating no difference between AS and RS. Additionally, for fiber-reinforced thermoplastic composites, the main

difficulty is the lack of continuity between fibers of BM and NZ. Moreover, Kiss and Czigány [53] performed stationary shoe FSW of 30% glasses fiber-reinforced composites and reported that this method could realize the homogenization and interlocking of fiber, as indicated in Fig. 13. A screwed pin with eight teeth reduced the length of fiber, which was the half than that of a screwed pin with four tooth, decreasing mechanical property. Fracture surface showed that fiber was extracted from the NZ, indicating interlocking each other inside the NZ (Fig. 13).

### 1.5.2 Double-pass and self-reacting friction stir welding

Aiming at the elimination of lack of root penetration and improvement of mechanical properties, Arici et al. [42, 54] proposed double-pass FSW to join MDPE sheet and expounded that double-pass FSW could successfully eliminate the lack of root penetration, as shown in Fig. 14a. Sound joint without inside defect was obtained using a tilting angle of  $1^\circ$  than 0. This was because the softened materials could be remained in the NZ. When tilting angle was higher than  $1^\circ$ , thickness reduction gradually increased, which decreased the area of load bearing, deteriorating joint quality. Moreover, the joining interface line was reduced, decreasing of tensile property. Under a welding speed of 12.5 mm/min, a rotational velocity of 1000 rpm and a tilting angle of  $1^\circ$ , maximum tensile strength of 20.45 MPa was attained, equivalent to 86.7% of BM. Fracture location lied at the HAZ, as shown in Fig. 11c and d. Saeedy et al. [55] performed double-pass FSW of 8 mm thick HDPE sheet and stated double-pass FSW improved tensile property compared with single-pass FSW significantly. The joint strength by double-pass FSW was twice than that using single-pass FSW. However, fracture of joint presented brittle fracture resulting from the decrease of crystallinity. Although double-pass FSW can solve the lack of root penetration, the surface formation is bad and the thickness reduction is serious. Furthermore, double-pass FSW process is still needed to be further optimized.

Besides double-pass FSW, Pirizadeh et al. [56] proposed self-reacting FSW (SRFSW) to eliminate root defect, which consisted of upper shoulder, lower shoulder and rotational pin, as indicated in Fig. 15. The gap between upper and lower shoulder

is approximately equivalent to thickness of sheet. During SRFSW process, the upper and lower shoulders, and rotational pin friction with welded materials, generating frictional heat and material flow, while the lower shoulder also acts as backing plate. Using the new tool, the lack of root penetration defect debilitating both tensile and bending strengths was eliminated. At a high rotational velocity or a low welding speed, the molten materials easily poured out of the NZ, and consequently lack of material caused low tensile strength. There is an optimum combination between welding speed and rotational velocity to reach maximum tensile strength (Table 2). Greater contacting area between a convex pin and sheets resulted in higher frictional heat and consequently better mixing of welded materials, and better distribution of temperature compared with a simple pin, which attributed to the better stability of the convex pin. At a welding speed of 40 mm/min and a rotational velocity of 400 rpm, the maximum values of the concave and simple pins were 20.7 MPa and 15.6 MPa, which reached the 60.6% and 45.6% of BM, respectively.

### 1.5.3 Submerged and additive friction stir welding

Polymers possess a low thermal conductivity (lower than  $0.5 \text{ Wm}^{-1}\text{K}^{-1}$ ), a short solidified time, and a low melting temperature than metal materials. During FSW of polymer, the low thermal conductivity causes that friction heat mainly concentrates in the NZ, creating a bigger temperature difference at the NZ. This causes that material flow is difficult to control. In order to solve uneven temperature distribution induced by low thermal conductivity and high cooling rates, Gao et al. [39, 57] proposed submerged FSW (SFSW) to improve homogeneity of temperature distribution. SFSW not only reduced peak temperature, but also effectively controlled thermal cycle, which in turn affected microstructural evolution. Maximum tensile strength of SFSW joint was 12.3 MPa, which was higher than that of conventional joint, while all the fractures located at the HAZ. The formations of crack and air bubbles as well as the decrease of crystalline content were major reasons of the decrease in tensile strength. Carbon nanotubes (CNTs) offer super high ductility, Young's modulus, strength and unique electrical properties as well as similar chain structure to polymers, especially

high thermal conductivities of 2800-6000  $\text{Wm}^{-1}\text{K}^{-1}$  at room temperature. Gao et al. [58] added multi-walled CNTs (MWCNTs) into the NZ during FSW of HDPE and ABS, and found that the addition of MWCNTs could increase thermal conductivity of NZ and then improve sufficient material flow and material mixture, reducing inside crack defect. The maximal tensile strength was 14.7 MPa, which could reach more than 65.3% of the parent HDPE. Shaikh et al. [59] investigated the effect of SiC,  $\text{SiO}_2$ , nano Al and graphite on mechanical property of HDPE joint. Compared with conventional FSW joint with tensile strength of 20.7 MPa and elongation of 60%, maximum tensile strength of SiC-reinforced composites reached 17.7 MPa, while elongation of graphite-reinforced composites up to 100%.

### 1.6 Brief summary

In summary, FSW has successfully joined different kinds of thermoplastic polymers and then obtain high joint strength by optimum combinations of welding tool and process parameters. However, the toughness is limited due to the voids at the RS and lack of root penetration. Although some new techniques such as stationary shoe FSW, SRFSW, SFSW and so on can reduce or eliminate these defects, the new processes are still immature and needed to be further optimized. Moreover, aiming at fiber-reinforced thermoplastic polymers, the smash and re-distribution of fiber as well as thermo-mechanical behavior during FSW need to be investigated. From the viewpoint of engineering application, fatigue performance of FSW joint is also very important.

## 2 Preparation of multifunctional polymer matrix composites

In last two decades, polymer matrix composites that exhibit the global properties of both fillers and polymers have been the subject of extensive research. Physical and mechanical properties of polymer matrix composites are very important and remarkably influenced by the structures and compositions of the molecular layers. The filler materials such as CNTs and Cu particles easily agglomerate in polymer, which are difficult to be separated due to van der Waals force [60, 61]. Therefore, the dispersion of fillers in polymer is the key issue to enhance the properties of polymer matrix composites. Currently, the primary techniques of preparing polymer matrix

composites are in situ polymerization [62], solution mixing [63] and melt blending [63], respectively.

In present, many attentions have been paid to a new composite fabrication technique named as friction stir processing (FSP). FSP derived from FSW is solid state process for microstructural modifications, fabrication of surface layer and bulk composites, which has potential to the mixing and joining of polymer molecules and filling materials together, based on low processing temperature, big shear force and stirring behavior (Fig. 16). FSP has been widely used to prepare metal matrix composites [18]. Up to present, FSP fabrication technology of multifunctional polymer matrix composites is proposed to improve mechanical property, electrical and thermal property of polymers [64].

### **2.1 In-situ friction stir processing**

Barmouz et al. [65] presented in-situ FSP fabrication nanoclay composites. A very good level of dispersion of nanoclay layers formed in the matrix, and many disordered single platelets were observed. Shear forces of FSP applied on the polymer macromolecules caused nanoclay layers to separate, increasing the ease of penetration of polymer chains into the silicate galleries. The higher the dispersion state and delamination of nanoclay layers, the higher elastic response of polymer nanocomposites and thus higher values of storage modulus. Moreover, a different opposing influences of welding speed could be responsible for hardness. The lower welding speed led to the longer time of stirring action, which resulted in an enhancement of dispersion of nanoclay and hardness. Increasing welding speed caused the NZ to be compressed which caused higher amounts of thermo-mechanical stress on the polymer and the improvement in dispersion state of nanoclay particles. Compared with HDPE, the hardness fabricated by FSP was improved by 62%, which was far higher than 22% obtained by melt mixing.

### **2.2 Stationary shoe friction stir processing**

A primary problem during FSP of polymer is to promote uniform cooling rates through the NZ. If outer layers of polymer cool much quicker than inner, a hard shell forms. As the inner layers cool, the materials contract and pull away from the shell.

Therefore, large voids form, which reduces mechanical and surface properties of fabricated composites. It is necessary to provide sufficient time to surface layers of polymers to cool and prevent the quenching of molten polymer crystals. Aiming at the disadvantages, Azarsa and Mostafapour [66] proposed a novel tooling system containing a rotational pin, a stationary shoe and a heating system located inside the stationary shoe, which was applied to produce HDPE/Cu composites from the viewpoint of improving electrical and thermal properties, as exhibited in Fig. 17. Good dispersion of Cu particles in the NZ and higher level of interfacial adhesion between copper particles and polymer matrix were achieved due to severe stirring action of pin, additional heat provided by shoulder and adequate pressure of designed tool system, obtaining high ultimate tensile strength and modulus of elasticity. Importantly, low welding speed resulted in low cooling rates, slow crystals growth and allowed polymer to crystallize, improving mechanical property. Under the synthetic effect of Cu fillers and the enhancement of transmission of phonon induced by high crystallinity, electrical properties of HDPE was enhanced significantly. Alyali et al. [67] employed a stationary shoe with heating system to fabricate PP/Al<sub>2</sub>O<sub>3</sub> composites. The heating system could keep uniform temperature distribution and cooling rates. FSP made the Al<sub>2</sub>O<sub>3</sub> particles dispersedly distribute in the NZ and then strengthened the BM. When a rotational velocity, a welding speed and a heating temperature were respectively 1000 rpm, 50 mm/min and 190 °C, the hardness and tensile strength of 4 with 15% Al<sub>2</sub>O<sub>3</sub> were improved by 54% and 6%, respectively. Farshbaf et al. [68] employed FSP to fabricate Nylon 6/MWCNTs composites and established finite element simulation based on Lagrangian incremental formulation. A good agreement between simulation predictions and actual observations was obtained. Peak temperature appeared at the interface of shoulder/workpiece. The more the distance from the center of the tool, the less the temperature at the NZ. Significantly, the flow behavior of Nylon 6 and dispersion pattern of MWCNTs were successfully predicted. MWCNTs was separated each other when the pin passed due to high plastic strain applied on them. Moreover, great amounts of materials accumulated in the AS of NZ after passing the pin. Krause et al. [69] also indicated that the presence of the



MWCNTs might further improve the compatibility of thermoplastic blends.

### **2.3 Submerged friction stir processing**

In addition, Gao et al. [70] prepared MWCNTs/HDPE composites employing submerged FSP to solve the problem that material flow is difficult to control induced by bigger temperature difference. Shear force that worked on the polymer materials was beneficial to disperse MWCNTs in the HDPE matrix, while the well-dispersed MWCNTs in a semi crystalline polymer matrix could lead to the increase of crystalline phases from the surface of the MWCNTs. This phenomenon was also reported by Deng et al. [71] that CNTs acted as an efficient nucleating agent on polymers and accelerated the crystallization process. The maximal tensile strength value of submerged FSP joint of 27 MPa, which was higher than HDPE matrix (22.5 MPa). According to the above-mentioned results, FSP is a practical way to fabricate multifunctional polymer matrix composites.

### **2.4 Brief summary**

Based on the advantages of low processing temperature, big shear force and stirring behavior, FSP can make reinforced phase dispersedly distribute at the polymer and high level of interfacial adhesion between reinforced phase and polymer matrix, has become the candidates to prepare multifunctional polymer matrix composites. Moreover, FSP can also realize selective processing of polymer sheet saving cost. However, material flow during FSP is extremely complex, which perhaps restricts uniform distribution of reinforced phase. Meanwhile, how to realize the preparation of large area sheet and the homogenization of reinforced phase at the interface between two or multi passes need to be further investigated.

## **3 Dissimilar friction stir welding of polymer and metal**

Global trends in CO<sub>2</sub> emission and gas price have attracted more and more attentions from the manufacturing fields of automotive, aviation, aerospace and so on, to produce lighter, safer and more environmental friendly vehicles. Especially, selection of light materials (i.e. aluminum, magnesium and polymers) can enormously realize the lightweight and reduction in emissions of greenhouse gases. In the field of new generation aircraft, the large multi-material structures of 50 wt% composites



mixed with 50 wt% lightweight metals have been largely used in the Boeing 787 Dreamliner and Airbus A350 XWB. The proportion of materials in Airbus A350XWB is shown in Fig. 18a. Moreover, in the automobiles, the Mercedes-Benz F125 research vehicle proposes a new concept under developments in the 2025 year and beyond, which contains polymer-metal hybrid structure to satisfy the emission-free mobility, as exhibited in Fig. 18b. Therefore, development and employment of hybrid structures of different materials with diverse ranges of properties require designers and engineers to select the proper joining methods of materials to fulfill the desired properties. FSW, involving temperature, mechanics, metallurgy and interaction, is solid state joining technology, which possesses the dual advantages of chemical bonds and mechanical interlocking. Up to present, FSW has become the candidate to join polymer and metal replacing conventional adhesive and mechanical joining methods [72-76]. The scholars in scientific communities and industries have published some satisfactory results, as exhibited in Table 6. Meanwhile, the adhesive bonding strength of metal-polymer in Table 6 was calculated by the ratio of the maximum load at failure/bonded area. The adhesive bonding results was calculated and summarized according to the reference [77], which contains the joints with and without surface pre-treatments.

### 3.1 Mechanical interlocking

Moshwan et al. [78-80] performed a preliminary study about FSW between 7075 alloy and PC sheet with the thickness of 3 mm using a welding tool whose diameters of shoulder and pin, pin length were 9 mm, 1 mm and 1 mm, respectively. 7075 alloy and PC sheet were successfully welded by frictional heat. 7075 alloy was transported (Fig. 19) and interlocked into PC sheet, but the ceramic-type (carbide, hydride or oxide) compound was absent. No diffusion occurred at joint interface. Mechanical interlocking of 7075 alloy and PC was the main joining mode, attributing to joint strength. At a plunging depth of 0.2 mm, a welding speed of 100 mm/min and a rotational velocity of 3250 rpm, tensile strength and elongation were respectively 4.72 MPa and 0.18% due to no significant mixture and diffusion.

Liu et al. [81] joined 6061 alloy and Nylon 6 using friction lap welding (FLW),

where 6061 alloy was placed at the upper and Nylon 6 located at the bottom. The FLW results showed no obvious welding distortion and warping because of low peak temperature, which may be attractive for structural applications in manufacturing industries owing to the saving cost and time required for distortion correcting. Under a rotational velocity 2000 rpm and a welding speed of 600 mm/min, tensile fracture did not fracture along the polymer-metal interface, but across the Nylon 6 sheet near the edge of the NZ, as shown in Fig. 20c. High quality lap joints with 5-8 MPa were obtained over a wide range of welding parameters. Increasing rotational velocity not only increased heat input, but also bended the 6061 alloy towards to Nylon 6. However, the bubbles occurred at the interface between metal and polymer, reducing the ability of load bearing and increasing stress concentration under cyclic loading. In order to obtain high strength hybrid joint without bubbles, Liu et al. [82] employed 800-grit sand papers to mechanical ground the surface of AZ31B sheet and joined with Nylon 6. The volume of bubbles was controlled by the amount of gases generated due to the pyrolysis of Nylon 6 and the amount of gases squeezed out of the joint during welding. The FLW joint strength was enhanced by reducing the volume of bubbles and increasing the surface roughness of AZ31B sheet.

Different from FLW, Ratanathavorn et al. [83, 84] used friction stir lap welding (FSLW) to produce shear overlap joint between 6111 alloy and Poly Phenylene Sulfide (PPS), in which a rotational pin was plunged into the lower sheet and created metallic chips merging with the molten polymer, fabricating metal-polymer joint. Macro mechanical locking formed between the chipped polymer filled zone and the surrounding aluminum sheet. Voids defect was detected at the boundary interface between re-solidified polymer and metal because of the big difference in thermal expansion coefficient. Excessive vertical flow of polymer matrix reduced the failure load under the cases of slow welding speed or big distances to backing of rotational pin tip. Additionally, fracture took place in two mechanisms, including initial fracture along the boundary between the aluminum and NZ, and fracture through polymer sheet. Shahmiri et al. [85] also showed a distinctive interaction layer at polymer/aluminum interface, which consisted of C, O and Al elements. Maximum

shear tensile strength of 5.1 MPa (~20% of polymer shear strength) was obtained, which was higher than or comparable to those of the joints produced by other processes. Shear strength of joint was significantly influenced by heat input, which decreased by increasing heat input because of the increase in the thickness of the interaction layer as well as the gap width between interaction layer with both aluminum and polymer matrices, induced by relative weak adhesion of the interaction layer to matrix, as shown in Fig. 19. Moreover, low joint strength at higher heat input might be attributed to thermal degradation, reduction in molecular weight caused by the decrease in the crystallinity of the polymer.

### **3.2 Effect of surface pre-treatment on adhesive mechanism**

As a matter of fact, metal and polymer can be joined together through Van der Waals force, chemical bonds (e.g. hydrogen bond and adhesive bond) and mechanical interlocking. Van der Waals force and hydrogen bond are very weak so that adhesive bond and mechanical interlocking are essential for achieving superior performance joint. As discussed above, although mechanical interlocking can be obtained by mixing both materials, the gap between metal and polymer easily appears because of big difference in the coefficient of thermal expansion, which is extremely difficult to form adhesive bonding at the interface between polymer and polished metal. At present, one of the important and extensive methods improving adhesive bonding by increasing surface energy is surface pre-treatment. This can guarantee that surface energy of the substrate should be higher or equal to the adhesive to achieve a complete wetting, good adhesion. Surface pre-treatment is mainly divided into three parts: mechanical pre-treatment, chemical pre-treatment and electrochemical pre-treatment.

#### **3.2.1 Mechanical and chemical pre-treatments**

Mechanical pre-treatment is mainly sandblasting (SB) or grit-blasting, which generates a macroscopically rough surface, promoting mechanical interlocking as the primary bonding mechanism between metal and polymer. The SB can also remove loose surface contaminations, increase effective surface area, improve wettability and

alter physicochemical state of aluminum surface. Chemical pre-treatment provides initial strength and durability superior to those from mechanical pre-treatment. Chemical pre-treatment is generally divided into two categories of acid etching (acid pickling) and conversion coating.

Yusof et al. [86, 87] performed friction stir spot welding (FSSW) of PET and 5052 alloy. Strong interfacial bonding between PET and 5052 alloy was attained due to higher surface roughness treated by chemical pre-treatment, which was superior than that by mechanical pre-treatment. Tensile shear failure load for an as-received surface ( $0.31 \mu\text{m Ra}$ ) specimen was about 0.4~0.8 kN while that for the treated surface ( $>0.31 \mu\text{m Ra}$ ) specimen was about 4.8~5.2 kN. This was because that when a liquid was applied to a rough surface, which filled the irregularities of the substrate surfaces, such as microgrooves, holes and dips, forming mechanical interlocking.

### 3.2.2 Electrochemical pre-treatment

Electrochemical pre-treatment has been extensively studied as a way to convert aluminum surface to aluminum oxide. The most common electrochemical pre-treatments for aluminum are [75]: chromic acid anodizing (CAA), phosphoric acid anodizing (PAA), sulfuric acid anodizing (SAA) and plasma electrolytic oxidation (PEO). All anodizing processes are multi-step procedures to achieve the desired properties of pre-treatment. CAA and PAA are the most often used pre-treatments in the aerospace industry.

Fig. 22 exhibits schematic diagram of formation of oxide layer on the aluminum surface after anodizing pre-treatment. A generated oxide forms a barrier layer on top surface of aluminum alloy to protect it against corrosion or humid environment. The thickness and morphology of the oxide layer depend on the applied voltage, time and relative resistivity. Moreover, the oxide layer at the top consists of a large number of microscopic open porosities. The homogeneous cell structure arranges in a closely packed hexagonal structure with open porosities in the center of the cells. Such a highly microporous structure increases micro-mechanical interlocking at the interface between the oxide layer and the molten polymer or adhesive, enhancing joint strength.

Meanwhile, the  $\text{Al}_2\text{O}_3$  layer easily produces covalent bond with the OH group, improving adhesive bonding.

Okada et al. [88] stated that HDPE was not able to be welded for as received 2017-T4 alloy, while anodizing was effective to join metal to polymer. A part of oxide layer was decomposed by hydrolysis to form hydroxyl group. This group reacted to functional groups of polymer and raised intermolecular force [11]. As ethylene-acrylic acid copolymer (EAA) has  $\text{COOH}$ , when polymer approaches aluminum, an intermolecular force arises between the natural oxide film on aluminum ( $\text{Al}_2\text{O}_3$ ) and  $\text{COOH}$ . In addition, Coulomb's forces between aluminum and oxygen, oxygen and hydrogen arise during welding, joining 2017 alloy and EAA tightly. Anodizing contributes to stable oxide layer on 2017 alloy and gives an anchor effect for which molten EAA permeated into depressions in anodized layer. On the contrary, as PE has no functional group, the intermolecular force is able to arise, but the coulomb's force is not able to arise, so the combination of as received 2017 alloy and PE is not able to join. However, when PE is coated with a porous film such as anodizing, it can be joined with sufficient strength due to an anchor effect.

Liu et al. [89] investigated the joining of magnesium alloy to PE without adhesive by FLW, in which the PE and magnesium alloy were hard to be joined together without surface pre-treatment due to the lack of polar groups on PE surface. Strong hybrid joint was achieved after PE was treated by corona discharge and magnesium alloy was subjected to plasma electrolytic oxidation (PEO) treatment. SEM and high resolution transmission electron microscope (HRTEM) observations demonstrated that the high joining strength was attributed to the development of both chemical bonds at the interface and micro-mechanical interlocking, as shown in Figs. 23 and 24. In addition, The HRTEM image also indicated that metal and polymer were tightly joined on the atomic or molecular level, which was beneficial to improve joint strength.

Aliasghari et al. [90] investigated effect of PEO pre-treatment on joining of 5052 alloy and PP using FSSW. The PEO treatment produced a thermally-insulating, porous ceramic coating, which was favorable for incorporating interlocking between

metal and molten polymer, as shown in Fig. 25. The bonding between polymer and alloy for the PEO-treated joint was superior compared with that of the untreated joint. The bonding in the PEO-coated specimen involved mechanical interlocking by flow of molten PP into open pores, cracks and cavities, associated with cohesive-adhesive fracture, whereas the untreated joint revealed an adhesive failure. However, thermal degradation of polymer was reported by the presence of carbonyl species in joint prepared by the PEO-coated alloy decreasing crystallinity of PP in joint due to the thermal insulating property of the PEO coating. Moreover, the formation of bubbles due to degradation of the PP during FSSW enhanced stress concentration within the PP in this region. The above two factors degraded tensile property. Therefore, it is emphasized the importance of an appropriate surface pre-treatment to optimize joint strength.

### **3.3 Limitation for friction stir welding of metal and polymer**

Owing to the big difference in melting points for metal and polymer, the bubbles easily form at the interface of metal and polymer, which reduce the ability of load bearing and increase stress concentration under cyclic loading, decreasing joint strength heavily. Yusof et al. [86, 87] stated that bubbles had two opposite effects: On one hand, the flow of bubbles pushed the softened PET into irregular rough surface to form mechanical interlocking, improving joint strength. On the other hand, the presence of the hollow at the joining interface prevented PET from contacting with 5052 alloy, while bubbles or hollows were crack source that induced crack paths, degrading the joint strength. Therefore, how to reduce or eliminate the bubbles will be an important research project.

### **3.4 New technique of friction spot joining for polymer and metal**

#### **3.4.1 Principles of friction spot joining**

Friction spot joining (FSpJ) is an alternative process developed and patented by Helmholtz-Zentrum Geesthacht in Germany for producing metal-polymer overlap joint. The principle of FSpJ is developed based on refill-FSSW technique which has been widely applied to spot joining of Al alloys or polymers [91-93]. Here, the

principle of FSpJ of polymer matrix composites and metal is briefly introduced. FSpJ employs a three-piece non-consumable tool system containing a clamping ring, a sleeve and a pin, respectively (Fig. 26a). Firstly, the rotational sleeve plunges to a pre-defined depth without reaching the composite beneath the metal (Fig. 26b), while the pin retracts upward. Under the synthesis actions of frictional heat generated between the metal and sleeve as well as axial forces exerted by the plunging motion of the sleeve, a volume of the plasticized metal around the tool flows into the cavity left behind by the retraction of the pin. Next, the pin pushes the plasticized metal to its original position (Fig. 26b). This results in the deformation of the metal sheet at the interface with the composite in the form of an undercut known as a metallic “nub”. As a result of the axial forces, the nub is slightly inserted into the composite leading to macro-mechanical interlocking between the joining parts. Simultaneously, the frictional heat is transferred from the metal to the composite via thermal conduction. This leads to the local increase of the temperature, exceeding melting temperature of the composite’s matrix, while a thin layer of the molten or softened polymer forms in the contacting area. A part of the molten layer is squeezed out and flows laterally throughout the overlap region as a result of axial pressure exerted by the tool. The molten layer is then consolidated under pressure, whereby it induces adhesion forces between the metal and composite. Finally, the tool retracts (Fig. 26b) and the spot join consolidates [94].

Fig. 26c demonstrates a sound, consolidated metal-composite joint. A typical cross-section prior to the failure of the joint and separation of the joining parts is shown in Fig. 26d. The metallic nub is indicated in the Fig. 26d at the metal composite interface. Compared with conventional FSSW [95-97], FSpJ owns many advantages no keyhole defect and obvious thickness reduction, big area of load bearing, no broken of reinforced fiber, short joining cycles, operation simplicity, excellent mechanical property and so on.

### 3.4.2 Process development of friction spot joining

Amancio-Filho et al. [98] firstly employed FSpJ to weld 2024-T3 alloy and



carbon-fiber-reinforced poly(phenylene sulfide). Thermo-mechanical phenomena associated with the FSpJ process enhanced metallurgical and polymer physical-chemical transformations. FSpJ joints with elevated tensile shear strength (20-28 MPa) were obtained without surface pre-treatment, higher than those of other welding techniques, as shown in Fig. 27. These positive preliminary results successfully indicated FSpJ is an alternative technology to produce hybrid polymer-metal structures. However, the bonding mechanisms of FSpJ are not yet well understood. Subsequently, Goushegir et al. [97] concluded the two main bonding mechanisms in FSpJ: (1) macro-mechanical interlocking due to the nub formation and (2) adhesion forces owing to the micro-scale filling of metal surface crevices and pores by molten polymer and partial exposed fiber entrapment by the plasticized metal at the interface.

Esteves et al. [99] systematically investigated hybrid 6181-T4 alloy/carbon fiber-reinforced PPS (CF-PPS) joint by Taguchi method and analysis of variance (ANOVA). Rotational velocity was the parameter with the largest influence on lap shear strength of joint (34.77%), followed by the joining time (32.37%), plunge depth (20.70%) and joining force (12.15%). The combination of rotational velocity and joining time increased heat generation, which was responsible for the amount of the molten PPS layer at the interface, increasing bonding area. Plunge depth plays an important role in the macro-mechanical interlocking at the metal-composite interface controlling the formation of the metallic nub. The higher the plunge depth, the more pronounced the metallic nub. At an optimum rotational velocity of 1200 rpm, a plunging depth of 1.15 mm, a joining time of 6 mm and a joining force of 8.3 kN, the ultimate shear forces were  $3523 \pm 527$  N.

Moreover, Esteves et al. [14] demonstrated the mechanical performance of joint by performing metal surface pre-treatment to increase adhesion forces could be increased approximately 160% in comparison to the as-received condition ( $708 \pm 55$  N for the as-received and  $1861 \pm 203$  N for the surface treated samples) during FSpJ of CF-PPS with 6181-T4 alloy. Failure mechanisms for the as-received and surface treated joints consisted of a mixture of cohesive and adhesive failures. In this type of



failure, the crack initiated at the end of the joined spot area and propagated parallel to lap interface between the metallic adhered and the adhesive layers until the beginning of the metallic nub volume; at this point a mixed regime of adhesive and cohesive failures started to take place. Considering that the metallic nub mechanically entrapped a volume involving fibers and polymer matrix, crack propagation tended to deviate to the consolidated molten layer in the composite and failure would be cohesive with partial fiber breakage, as displayed in Fig. 28. Goushegir et al. [100] performed FSpJ on 2024-T3 alloy and CF-PPS. The changes of process-related physicochemical in the composite were studied through thermal analysis methods of DSC and Thermo Gravimetric Analyzer (TGA) which suggested no extensive thermal degradation occurred during FSpJ process. The PAA pre-treatment specimen showed the highest mechanical strength since the carbon-based primer layer formed a strong, primary C-C chemical bonding with the molten PPS layer. Moreover, PAA electrochemical pre-treatment led to a highly porous oxide layer that increased micromechanical interlocking between the molten PPS and the oxide layer. The radial cracks nucleated at the periphery of the bonding area and propagated rapidly until failure of the so-called adhesion zone. Upon further loading, the crack propagated into the transition and plastically deformed zones, leading to a reduction of the stiffness.

### 3.5 Brief summary

As mentioned above, thermoplastic polymer and metal can be successfully joined by FSW, FLW, FSLW or FSpJ, and then achieve the satisfactory results. However, bubbles, degradation and gap occurred at the interface of metal and polymer can reduce the ability of load bearing and increase stress concentration under cyclic loading, decreasing mechanical property. In order to expend the engineering application, the optimum surface pre-treatment need to be groped to avoid these disadvantages, while fatigue performance reacting the reliable of structural design shall be explored.

## 4 Conclusion and future outlook

In this paper, the current studies for FSW/P related to thermoplastic polymers/polymer matrix composites (welding process variables, thermo-mechanical

behavior, mechanical properties and new FSW techniques eliminating welding defects), fabrication of multifunctional composites as well as dissimilar FSW of metal and polymer are reviewed.

FSW has the potential to join thermoplastic polymers/polymer matrix composites replacing other welding techniques. Sound joint with high quality can be obtained by regulating and controlling welding process variables or changing preheating modes. Low thermal conductivity and crystallinity are main factors decreasing mechanical properties, while the voids on the RS and lack of root penetration are main defects during FSW of polymer. By employing new FSW methods such as stationary shoe with preheating system, self-reacting tool and submerged FSW, the good material flow, low cooling rates and high crystallinity can be obtained, which are beneficial to the improvement of mechanical properties. FSP characterized by big shear stress possesses many advantages to fabricate polymer matrix composites. Moreover, the severe stirring and relative low peak temperature of FSW can make macro/micro mechanical interlocking and adhesive bonding between metal and polymer, revealing huge benefits for joining metal and polymer.

Despite the FSW of polymers has attained period results, the relevant research object is still in the feasibility. Some areas need to be addressed and these are:

(1) Thermal-mechanical and material flow behaviors

Thermal-mechanical and material flow behaviors are quite complex because of high peak temperature and big shear force, which significantly influence the formation of the voids between the TMAZ and NZ of RS and then affect mechanical properties. Several researchers suggest that the mechanisms of material transfer and bonding are characterized through the experimental investigations. Theoretical and numerical computational models may be beneficial to realize material flow during FSW of polymer and then reduce or eliminate the voids between the TMAZ and NZ of RS.

(2) Process development

Because of low thermal conductivity of polymer, lack of root penetration defect appears at the bottom, deteriorating mechanical properties. A hybrid stationary shoe

with pre-heating system on both crown and backing sides combined with optimized process parameters can preheat polymers, eliminating lack of root penetration and improving joint quality.

### (3) Crystallization behavior and evolution of molecular chains

The degree of crystallization and evolution of molecular chains during FSW of polymer play significant influences on joint formation and strength, which have not been investigated in detail. A better knowledge on crystallization behavior and evolution of molecular chains under high peak temperature and big shear forces is essential, which can provide significant reference for optimizing process parameter configuration, obtaining high quality joint. Meanwhile, aiming at polymer matrix composites, the effect of reinforced fiber on heat generation as well as the broken and re-distribution of reinforced fiber need to be explored.

### (4) FSW/P of MWCNTs or graphene reinforced polymer matrix composites

MWCNTs or graphene offers super high ductility, Young's modulus, strength and unique electrical properties, which possesses multi-advantages during FSW/P, such as accelerating the crystallization process, increasing thermal conductivity, improving adhesive bonding as bridge. Therefore, investigating the effect of reinforced phase on crystallization behavior, material flow especially on the RS, reinforced mechanism during FSW/P of polymers shall be required.

### (5) Dissimilar FSW of polymers or polymer and metal

FSW provides big shear stress and stirring actions, which has potential to join dissimilar materials (polymer and polymer or polymer and metal), satisfying the optimal allocation of structural properties. Especially aiming at dissimilar FSW of polymer and metal, optimal surface pre-treatment need to be groped to avoid the gap between molten polymer and metal, and then achieve strong hybrid joint. Meanwhile, the interface joining mechanism of metal and polymer should be further comprehended to regulate and control welding process.

## Acknowledgements

The work was jointly supported by the National Natural Science Foundation of

China (No. 51575132) and the Fund of National Engineering and Research Center for Commercial Aircraft Manufacturing (No. COMAC-SFGS-2016-33214).

## References

- [1] Strand SR. Effects of friction stir welding on polymer microstructure. Brigham Young University; 2004.
- [2] Barmouz M, Shahi P, Asadi P. Friction stir welding/processing of polymeric materials. *Advances in Friction Stir Welding and Processing*. 2014;601-670.
- [3] Pramanik A, Basak AK, Dong Y, Sarker PK, Uddin MS, Littlefair G, Dixit AR, Chattopadhyaya S. Joining of carbon fibre reinforced polymer (CFRP) composites and aluminium alloys: A review. *Compos Part A-APPL S*, 2017; 101:1-29.
- [4] Mostafapour A, Taghizad Asad F. Investigations on joining of Nylon 6 plates via novel method of heat assisted friction stir welding to find the optimum process parameters. *Sci Technol Weld Joi* 2016;21: 660-669.
- [5] Mishra RS, Ma ZY. Friction stir welding and processing. *Mater Sci Eng R* 2005;50:1-78.
- [6] Eslami S, Tavares, PJ, Moreira PMGP. Friction stir welding tooling for polymers: review and prospects. *Int J Adv Manuf Technol* 2016;89:1677-1690.
- [7] Clark J. Friction stir welding of polymeric materials. Utah: Brigham Young University; 1999.
- [8] Gao JC, Cui XX, Liu C, Shen YF. Application and exploration of friction stir welding/processing in plastics industry. *Mater Sci Technol* 2017;33:1145-1158.
- [9] Saeedy S, Givi MKB. Investigation of the effects of critical process parameters of friction stir welding of polyethylene. *Proceedings of the Institution of Mechanical Engineers. Part B: J. Eng Manuf* 2011;225:1305-1310.
- [10] Kusharjanta B, Raharjo WP, Triyono. Temperature comparison of initial, middle and final point of polypropylene friction stir welded. *AIP Conf Proceed* 2016;1717:040011.
- [11] Lambiasi F, Paoletti A, Di Ilio A. Effect of tool geometry on mechanical behavior of friction stir spot welds of polycarbonate sheets. *Int J Adv Manuf Technol* 2016;88:3005-3016.
- [12] Sadeghian N, Besharati G, Mohammad K. Experimental optimization of the mechanical properties of friction stir welded Acrylonitrile Butadiene Styrene sheets. *Mater Des* 2015;67:

145-153.

[13] Simões F, Rodrigues DM. Material flow and thermo-mechanical conditions during Friction Stir Welding of polymers: Literature review, experimental results and empirical analysis. *Mater Des* 2014;59:344-351.

[14] Zafar A, Awang M, Khan SR, Emamian S. Investigating friction stir welding on thick Nylon 6 plates. *Weld J* 2016;95:210S-128S.

[15] Kiss Z, Czigány T. Effect of welding parameters on the heat affected zone and the mechanical properties of friction stir welded poly(ethylene-terephthalate-glycol). *J Appl Polym Sci* 2012;125:2231-2238.

[16] Payganeh GH, Mostafa Arab NB, Dadgar Asl Y, Ghasemi FA, Saeidi Boroujeni M. Effects of friction stir welding process parameters on appearance and strength of polypropylene composite welds. *Int J Phy Sci* 2011;6:4595-4601.

[17] Ahmadi H, Mostafa Arab N B, Ghasemi FA. Optimization of process parameters for friction stir lap welding of carbon fibre reinforced thermoplastic composites by Taguchi method. *J. Mech Sci Technol* 2014;28:279-284.

[18] Sharma V, Prakash U, Kumar BVM. Surface composites by friction stir processing: A review. *J Mater Process Technol* 2015;224: 117-134.

[19] Balasubramanian V. Relationship between base metal properties and friction stir welding process parameters. *Mater Sci Eng A* 2008;480:397-403.

[20] Heidarzadeh A, Jabbari M, Esmaily M. Prediction of grain size and mechanical properties in friction stir welded pure copper joints using a thermal model. *Int J Adv Manuf Technol* 2014; 77:1819-1829.

[21] Xu N, Ueji R, Fujii H. Enhanced mechanical properties of 70/30 brass joint by rapid cooling friction stir welding. *Mater Sci Eng A* 2014;610:132-138.

[22] Aydin M. Effects of welding parameters and pre-heating on the friction stir welding of UHMW-polyethylene. *Polym-Plast Technol Eng* 2010;49:595-601.

[23] Bozkurt Y. The optimization of friction stir welding process parameters to achieve maximum tensile strength in polyethylene sheets. *Mater Des* 2012;35:440-445.

[24] Mendes N, Loureiro A, Martins C, Neto P, Pires NJ. Morphology and strength of acrylonitrile butadiene styrene welds performed by robotic friction stir welding. *Mater Des*

2014;64:81-90.

[25] Mendes N, Loureiro A, Martins C, Neto P, Pires NJ. Effect of friction stir welding parameters on morphology and strength of acrylonitrile butadiene styrene plate welds. *Mater Des* 2014;58:457-464.

[26] Jaiganesh V, Maruthu B, Gopinath E. Optimization of process parameters on friction stir welding of high density polypropylene plat. *Pro Eng* 2014;97:1957-1965.

[27] Hoseinlghab S, Mirjavadi SS, Sadeghian N, Jalili I, Azarbarmas M, Besharati Givi M K. Influences of welding parameters on the quality and creep properties of friction stir welded polyethylene plates. *Mater Des* 2015;67:369-378.

[28] Ji SD, Huang RF, Meng XC, Zhang LG, Huang YX. Enhancing friction stir weldability of 6061-T6 Al and AZ31B Mg alloys assisted by external non-rotational shoulder. *J Mater Eng Perform* 2017;26:2359-2367.

[29] Panneerselvam K, Lenin K. Investigation on effect of tool forces and joint defects during FSW of polypropylene plate. *Proc Eng* 2012;38:3927-3940.

[30] Lenin K, Abdul Shabeer H, Suresh kumar K, Panneerselvam K. Process parameters optimization for friction stir welding of Polypropylene material using Taguchi's approach. *J Sci Indus Res* 2014, 73, 369-374.

[31] Panneerselvam K, Lenin K. Study on hardness and micro structural characterization of the friction stir welded Nylon 6 plate. *Int J Mech Eng* 2013;2:51-62.

[32] Panneerselvam K, Lenin K. Joining of Nylon 6 plate by friction stir welding process using threaded pin profile. *Mater Des* 2014;53:302-307.

[33] Padmanaban G, Balasubramanian V. Selection of FSW tool pin profile, shoulder diameter and material for joining AZ31B magnesium alloy-An experimental approach. *Mater Des* 2009; 30:2647-2656.

[34] Elangovan K, Balasubramanian V, Valliappan M. Influences of tool pin profile and axial force on the formation of friction stir processing zone in AA6061 aluminium alloy. *Int J Adv Manuf Technol* 2007;38:285-295.

[35] Kiss Z, Czigan T. Microscopic analysis of the morphology of seams in friction stir welded polypropylene. *Exp Polym Lett* 2012;6:54-62.

[36] Vijendra B, Sharma A. Induction heated tool assisted friction-stir welding (i-FSW): A

novel hybrid process for joining of thermoplastics. *J Manuf Pro* 2015;20:234-244.

[37] Squeo EA, Bruno G, Guglielmotti A, Quadrini F. Friction stir welding of polyethylene sheets. *The Annals of Dunarea de Jos University of Galati, Technologies in Machine Building*. 2009;5:241-246.

[38] Ahmadi H, Arab NBM, Ghasemi FA, Farsani RE. Influence of pin profile on quality of friction stir lap welds in carbon fiber reinforced polypropylene composite. *Int J Mech App* 2012; 2:24-28.

[39] Gao JC, Shen YF, Zhang JQ, Xu HS. Submerged friction stir weld of polyethylene sheets. *J App Polym Sci* 2014;131:1-8.

[40] Abibe AB, Sônego M, dos Santos JF, Canto LB, Amancio-Filho ST. On the feasibility of a friction-based staking joining method for polymer–metal hybrid structures. *Mater Des* 2016; 92:632-642.

[41] Tan XH, Zhang J, Shan JG, Yang SL, Ren JL. Characteristics and formation mechanism of porosities in CFRP during laser joining of CFRP and steel. *Compos Part B-Eng* 2015;70:35-43.

[42] Arici A, Selale S. Effects of tool tilt angle on tensile strength and fracture locations of friction stir welding of polyethylene. *Sci Technol Weld Joi* 2013;12:536-539.

[43] Mostafapour A, Azarsa E. A study on the role of processing parameters in joining polyethylene sheets via heat assisted friction stir welding: Investigating microstructure, tensile and flexural properties. *Int J Phy Sci* 2012;7:647-654.

[44] Azarsa E, Asl AM, Tavakolkhah V. Effect of process parameters and tool coating on mechanical properties and microstructure of heat assisted friction stir welded polyethylene sheets. *Adv Mater Res* 2012;445:765-770.

[45] Azarsa E, Mostafapour A. Experimental investigation on flexural behavior of friction stir welded high density polyethylene sheets. *J Manuf Process* 2014;16:149-155.

[46] Mendes N, Neto P, Simão M, Loureiro A, Pires JN. A novel friction stir welding robotic platform: welding polymeric materials. *Int J Adv Manuf Technol* 2014;85:37-46.

[47] Rahbarpour R, Azdast T, Rahbarpour H, Shishavan SM. Feasibility study of friction stir welding of wood-plastic composites. *Sci Technol Weld Joi* 2014;19:673-681.

[48] Rezgui MA, Ayadi M, Cherouat A, Hamrouni K, Zghal A, Bejaoui S. Application of



Taguchi approach to optimize friction stir welding parameters of polyethylene. EPJ Web of Conferences 2010;6:07003.

[49] Eslami S, Ramos T, Tavares, PJ, Moreira PMGP. Shoulder design developments for FSW lap joints of dissimilar polymers J Manuf Process 2015;20:15-23.

[50] Eslami S, Ramos T, Tavares PJ, Moreira PMGP. Effect of friction stir welding parameters with newly developed tool for lap joint of dissimilar polymers. Pro Eng 2015;114:199-207.

[51] Rezaee Hajideh M, Farahani M, Alavi SAD, Molla Ramezani N. Investigation on the effects of tool geometry on the microstructure and the mechanical properties of dissimilar friction stir welded polyethylene and polypropylene sheets. J Manuf Process 2017;26:269-279.

[52] Kiss Z, Czigány T. Applicability of friction stir welding in polymeric materials. Mechanic Eng 2007;51:15-18.

[53] Czigány T, Kiss Z. Friction stir welding of fibre reinforced polymer COMPO composites. Proceeds 18th International Conference on Composites Materials. 2011.

[54] Arici A, Sinmaz T. Effects of double passes of the tool on friction stir welding of polyethylene. J Mater Sci 2005;40:3313-3316.

[55] Saeedy S, Besharati Givi MK. Experimental investigation of double side friction stir welding (FSW) on high density polyethylene blank. Proceedings of the ASME 2010 10th Biennial Conference on Engineering Systems Design and Analysis. Istanbul,Turkey. 2010;12-14.

[56] Pirizadeh M, Azdast T, Rash Ahmadi S, Mamaghani Shishavan S, Bagheri A. Friction stir welding of thermoplastics using a newly designed tool. Mater Des 2014;54:342-347.

[57] Gao JC, Shen YF, Xu HS. Investigations for the mechanical, macro-, and microstructural analyses of dissimilar submerged friction stir welding of acrylonitrile butadiene styrene and polycarbonate sheets. Proceed Institut Mechanic EngPart B: J Eng Manuf 2015;230:1213-1220.

[58] Gao JC, Li C, Shilpakar U, Shen YF. Improvements of mechanical properties in dissimilar joints of HDPE and ABS via carbon nanotubes during friction stir welding process. Mater Des 2015;86: 289-296.

[59] Shaikh AS, Tahir MS, Qureshi MKA. Experimental investigation of mechanical



properties of friction stir welded HDPE with additions of silicon carbide, silica, nano-alumina, and graphite. *Joi Adv Spec Mater* 2016;316-323.

[60] Atieh MA. Effect of functionalize carbon nanotubes with amine functional group on the mechanical and thermal properties of styrene butadiene rubber. *J Thermoplas Compos Mater* 2011;24:613-624.

[61] Zou YB, Feng YC, Wang L, Liu XB. Processing and properties of MWNT/HDPE composites. *Carbon* 2004;42:271-217.

[62] Wang F, Zhang Y, Zhang BB, Hong RY, Kumar MR, Xie CR. Enhanced electrical conductivity and mechanical properties of ABS/EPDM composites filled with graphene. *Compos Part B-Eng* 2015; 83:66-74.

[63] Mohan VB, Jayaraman K, Bhattacharyya D. Hybridization of graphene-reinforced two polymer nanocomposites. *Int J Smart Nano Mater* 2016;7:179-201.

[64] Prasad RV, Madhu Raghava P. Fsw of polypropylene reinforced with Al<sub>2</sub>O<sub>3</sub> nano composites, effect on mechanical and microstructural properties. *Int J Eng Res App* 2012;2: 288-296.

[65] Barmouz M, Seyfi J, Kazem Besharati Givi M, Hejazi I, Davachi SM. A novel approach for producing polymer nanocomposites by in-situ dispersion of clay particles via friction stir processing. *Mater Sci Eng A* 2011;528:3003-3006.

[66] Azarsa E, Mostafapour A. On the feasibility of producing polymer–metal composites via novel variant of friction stir processing. *J Manuf Process* 2013; 15: 682-688.

[67] Alyali S, Mostafapour A, Azarsa E. Fabrication of PP/AL<sub>2</sub>O<sub>3</sub> surface nanocomposites via novel friction stir processing approach. *Int J Adv Eng Technol* 2012;3:598-605.

[68] Farshbaf Zinati R, Razfar MR, Nazockdast H. Numerical and experimental investigation of FSP of PA 6/MWCNT composite. *J Mater Process Technol.* 2014; 214:2300-2315.

[69] Krause B, Schneider C, Boldt R, Weber M, Park HJ, Pötschke P. Localization of carbon nanotubes in polyamide 6 blends with non-reactive and reactive rubber. *Polymer* 2014;55: 3062-3067.

[70] Gao JC, Shen YF, Li C. Fabrication of high-density polyethylene/multiwalled carbon nanotube composites via submerged friction stir processing. *J Thermoplas Compos Mater* 2017; 30:241-254.

- [71] Deng SL, Lin ZD, Xu BF, Lin HB, Du CM. Effects of carbon fillers on crystallization properties and thermal conductivity of poly(phenylene sulfide). *Polym-Plast Technol Eng* 2015;54:1017-1024.
- [72] Kah P, Suoranta R, Martikainen J, Magnus C. Techniques for joining dissimilar materials: metals and polymers. *Rev Adv Mater Sci* 2014;36:152-164.
- [73] Ratanathavorn W. Hybrid joining of aluminum to thermoplastics with friction stir welding. Stockholm, Sweden: KTH-Royal Institute of Technology.
- [74] Patel AR, Dalwadi CG. A review: dissimilar material joining of metal to polymer using friction stir welding (FSW). *Int J Sci Technol Eng* 2016;2:702-706.
- [75] Nagatsuka K, Yoshida S, Tsuchiya A, Nakata K. Direct joining of carbon-fiber-reinforced plastic to an aluminum alloy using friction lap joining. *Compos Part B Eng* 2015;73:82-88.
- [76] Khodabakhshi F, Haghshenas M, Sahraeinejad S, Chen J, Shalchi B, Li J. Microstructure-property characterization of a friction-stir welded joint between AA5059 aluminum alloy and high density polyethylene. *Mater Charact* 2014;98:73-82.
- [77] Boone MJ. Mechanical testing of epoxy adhesives for naval applications. University of Maine, Orono, USA, 2002, 40-88.
- [78] Rahmat SM, Hamdi M, Yusof F, Moshwan R. Preliminary study on the feasibility of friction stir welding in 7075 aluminium alloy and polycarbonate sheet. *Mater Res Innov* 2014; 18:S6-515-S6-9.
- [79] Moshwan R, Firman R, Yusof F, Hassan MA, Hamdi M, Fadzil M. Dissimilar friction stir welding between polycarbonate and AA 7075 aluminum alloy. *Int J Mater Res* 2015;106:258-266.
- [80] Moshwan R, Firman R, Yusof F, Hassan MA, Hamdi M, Fadzil M. Dissimilar friction stir welding between polycarbonate and AA 7075 aluminum alloy. *Int J Mater Res* 2015;106:1-9.
- [81] Liu FC, Liao J, Nakata K. Joining of metal to plastic using friction lap welding. *Mater Des* 2014; 54: 236-244.
- [82] Liu FC, Nakata K, Liao J, Hirota S, Fukui H. Reducing bubbles in friction lap welded joint of magnesium alloy and polyamide. *Sci Technol Weld Joi*. 2014; 19(7): 578-587.
- [83] Ratanathavorn W. Hybrid joining of aluminum to thermoplastics with friction stir

welding. Stockholm, Sweden: KTH-Royal Institute of Technology; 2015.

[84] Ratanathavorn W. Development and evaluation of hybrid joining for metals to polymers using friction stir welding. Stockholm, Sweden: KTH Royal Institute of Technology; 2015.

[85] Shahmiri H, Movahedi M, Kokabi AH. Friction stir lap joining of aluminium alloy to polypropylene sheets. *Sci Technol Weld Joi* 2016;22:120-126.

[86] Yusof F, Miyashita Y, Seo N, Mutoh Y, Moshwan R. Utilising friction spot joining for dissimilar joint between aluminium alloy (A5052) and polyethylene terephthalate. *Sci Technol Weld Joi* 2013;17:544-549.

[87] Yusof F, Muhamad M, Moshwan R, Jamaludin M, Miyashita Y. Effect of surface states on joining mechanisms and mechanical properties of aluminum alloy (A5052) and Polyethylene Terephthalate (PET) by dissimilar friction spot welding. *Metals* 2016; 6:101.

[88] Okada T, Uchida S, Nakata K. Direct joining of aluminum alloy and plastic sheets by friction lap processing. *Mater Sci Forum* 2014;794-796:395-400.

[89] Liu FC, Liao J, Gao Y, Nakata K. Effect of plasma electrolytic oxidation coating on joining metal to plastic. *Sci Technol Weld Joi* 2015;20:291-296.

[90] Aliasghari S, Ghorbani M, Skeldon P, Karami, H, Movahedi M. Effect of plasma electrolytic oxidation on joining of AA 5052 aluminium alloy to polypropylene using friction stir spot welding. *Surf Coat Technol* 2017;313:274-281.

[91] Junior WS, Emmler T, Abetz C, Handge UA, dos Santos JF, Amancio-Filho ST. Friction spot welding of PMMA with PMMA/silica and PMMA/silica-g-PMMA nanocomposites functionalized via ATRP. *Polymer* 2014;55:5146-5159.

[92] Junior WS, Handge UA, dos Santos JF, Abetz V, Amancio-Filho ST. Feasibility study of friction spot welding of dissimilar single-lap joint between poly(methyl methacrylate) and poly(methyl methacrylate)-SiO<sub>2</sub> nanocomposite. *Mater Des* 2014; 64:246-250.

[93] Oliveira PHF, Amancio-Filho ST, dos Santos JF, Hage E. Preliminary study on the feasibility of friction spot welding in PMMA. *Mater Lett* 2010; 64:2098-2101.

[94] Goushegir SM, dos Santos JF, Amancio-Filho ST. Failure and fracture micro-mechanisms in metal-composite single lap joints produced by welding-based joining techniques. *Compos Part A* 2016;81:121-128.

[95] Arici A, Mert S. Friction Stir Spot Welding of Polypropylene. *J Reinf Plast Comp* 2008;

27:2001-2004.

[96] Bilici MK. Application of Taguchi approach to optimize friction stir spot welding parameters of polypropylene. *Mater Des* 2012;35:113-119.

[97] Yang XW, Fu T, Li WY. Friction Stir Spot Welding: A Review on joint macro- and microstructure, property, and process modelling. *Adv Mater Sci Eng* 2014;2014:1-11.

[98] André NM, Goushegir SM, dos Santos JF, Canto LB, Amancio-Filho ST. Friction Spot Joining of aluminum alloy 2024-T3 and carbon-fiber-reinforced poly(phenylene sulfide) laminate with additional PPS film interlayer: Microstructure, mechanical strength and failure mechanisms. *Compos Part B Eng* 2016;94:197-208.

[99] Esteves JV, Goushegir SM, dos Santos JF, Canto LB, Hage E, Amancio-Filho ST. Friction spot joining of aluminum AA6181-T4 and carbon fiber-reinforced poly(phenylene sulfide): Effects of process parameters on the microstructure and mechanical strength. *Mater Des* 2015; 66:437-445.

[100] Goushegir SM. Friction Spot Joining of Metal-Composite Hybrid Structures. Technische Universität Hamburg, 2015.

## Figure captions

Fig. 1 Schematic diagram of FSW

Fig. 1 Key factors affecting joint quality of FSWed polymer [18].

Fig. 2 (a) Representation of deformation zones and flow material for FSW of metals according Arbogast model and (b) Cross-section macrostructure [13].

Fig. 3 FSW of Nylon 6 polymer: (a) welding tool, (b) macrostructure of typical joint; material flow behaviors of (c) X-axis (parallel to the WD), (d) Y-axis (perpendicular to the WD) and (e) Z-axis (through the thickness direction) [14].

Fig. 4 Maximum tensile strength of FSW joint of polymer in published papers [40].

Fig. 5 Comparison of joint efficiency of PP welded joints using different welding techniques [1].

Fig. 6 DSC curves of PE in different conditions: (a) BM, (b) HAZ, (c) TMAZ and (d) NZ [41].

Fig. 7 Macrostructure of typical stationary shoes FSW joint of PP polymer [1].

Fig. 8 (a) Stationary shoe and (b) Schematic of designed fixture for heat assisted FSW [4].

Fig. 9 (a) Robotic FSW platform and (b) FSW tool [51].

Fig. 10 FSW tool with stationary shoulder: (a) design drawing, (b) actual tool, (c) Teflon stationary shoulder with brass and copper sleeves and (d) joint by Teflon stationary shoulder [47].

Fig. 11 Microstructures of FSW joint of PP [36].

Fig. 12 Welded zone in fiber reinforced composites with thermoplastic matrix: (a) non-intermeshing fibers and (b) intermeshing fibers at the interface; (c) borderline of the NZ and the BM and (d) fractured surface [55].

Fig. 13 Double-pass FSW: (a) schematic diagram, (b) macrostructure, (c) schematic and (d) actual of fracture location [56].

Fig. 14 SRFSW process: (a) exploded view of the new tool, (b) fixture and tool; schematic illustration of SRFSW: (c) tool starts rotation, (d) tool moves into material, (e) tool is attached to material and starts welding and (f) end of the welding and tool is out of the workpiece [58].

Fig. 15 Schematic diagram of multifunctional composites FSP fabrication technology: (a) by groove (b) by drilled holes (c) by using cover plate [18].

Fig. 16 FSP of HDPE/Cu composites: (a) schematic illustration of stationary shoes with heating system, (b) surface appearance, (c) macrostructure and (d) uniform dispersed Cu particles [69].

Fig. 17 Potential application for FSW of polymer and metal materials: (a) materials breakdown in Airbus A350XWB and (b) mercedes-Benz F125 research vehicle concept [80, 81].

Fig. 18 SEM image of cross-section joint interface for PC-7075 alloy of typical joint [88].

Fig. 19 Typical FLW joint processed using tool with dimension of 20 mm in diameter [82].

Fig. 20 (a) Schematic diagram; FE-SEM images of polymer/metal interface at different regions: (b) cross-section of typical joint at 800 rpm-70 mm/min, (c) region A, (d) region B, (e) region C and (f) interface of polymer/metal for 1200 rpm-70 mm/min joint [86].

Fig. 21 Schematic illustration of aluminum oxide after PAA pre-treatment, adapted from, and the proposed model of pore filling by the PPS. (1) complete wetting and pore filling, (2) complete wetting, incomplete pore filling, (3) partial wetting and incomplete pore filling, and (4) no wetting and no pore filling [80].

Fig. 22 Cross-section of FLW joint with highest USS of 4.67 MPa: (a) secondary electron imaging; (b) Mg, (c) O and (d) C atom distributions [93].

Fig. 23 TEM observation across FLW joint with highest USS of 4.67 MPa: (a) interface between Mg substrate and PEO film; high resolution TEM image of (b) region I, (c) region II and (d) region III; (e) interface between PEO film and PE; high resolution TEM image of (f) region IV, (g) region V and (g) region VI [93].

Fig. 24 (a) Scanning electron micrographs of (a) the surface and (b) the cross-section of 5052 alloy following PEO for 10 min in the silicate-based electrolyte [94].

Fig. 25 (a) FSpJ tool (dimensions are in mm); (b) Process steps: (1) the sleeve plunging softens the metal, (2) spot refilling, and (3) joint consolidation; (c) Top view of sound FSpJ joint after consolidation and (d) a typical cross-section indicating the metallic nub [98].

Fig. 26 Histogram showing average ultimate shear strength of selected FSpJ joints and available techniques (UW: ultrasonic welding, IW: induction welding, RW: resistance welding, FSSW: friction stir spot welding, AD: direct adhesive bonding) [99].

Fig. 27 Schematic illustration of the proposed crack propagation mechanism in friction spot joints under shear loading [100].

**Table captions**

Table 1 Comparison of process requirements for polymer joining methods for 12 in. long butt weld in 0.25 in. thick PP [1].

Table 2 Optimum combination of rotational velocity and welding speed for FSW of polymers.

Table 3 Welding tools used in the published papers during conventional FSW of polymer.

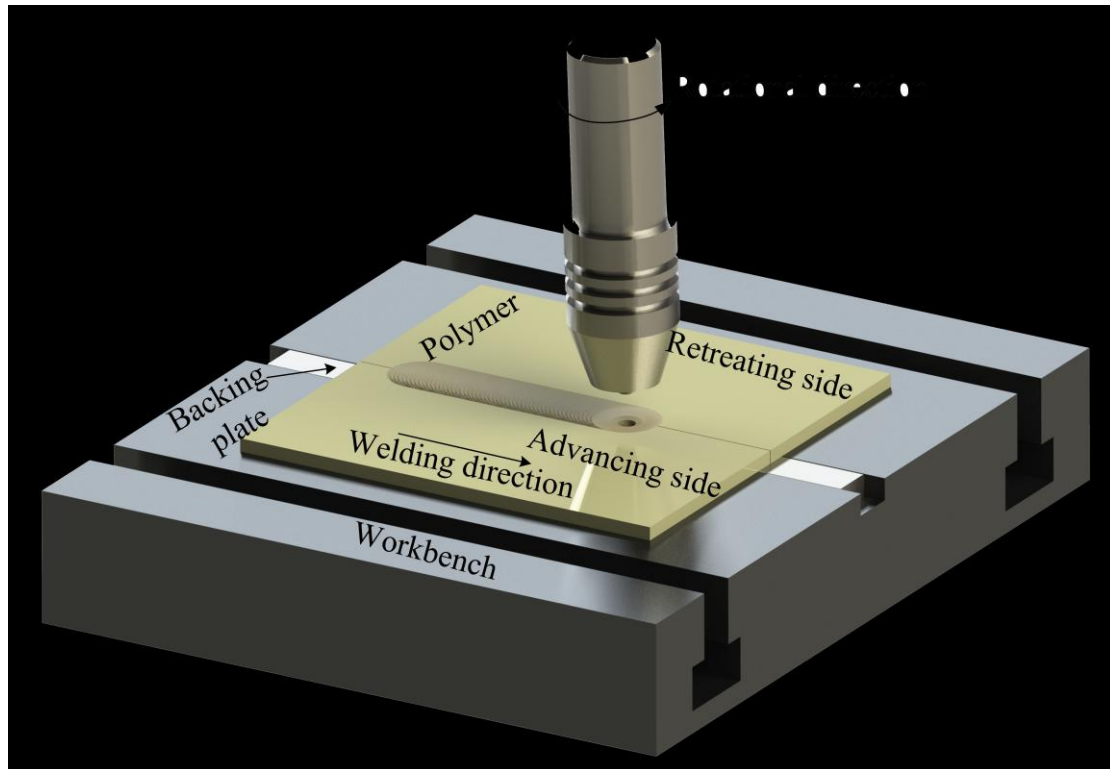
Table 4 Typical defects appeared at the joint during FSW of polymer.

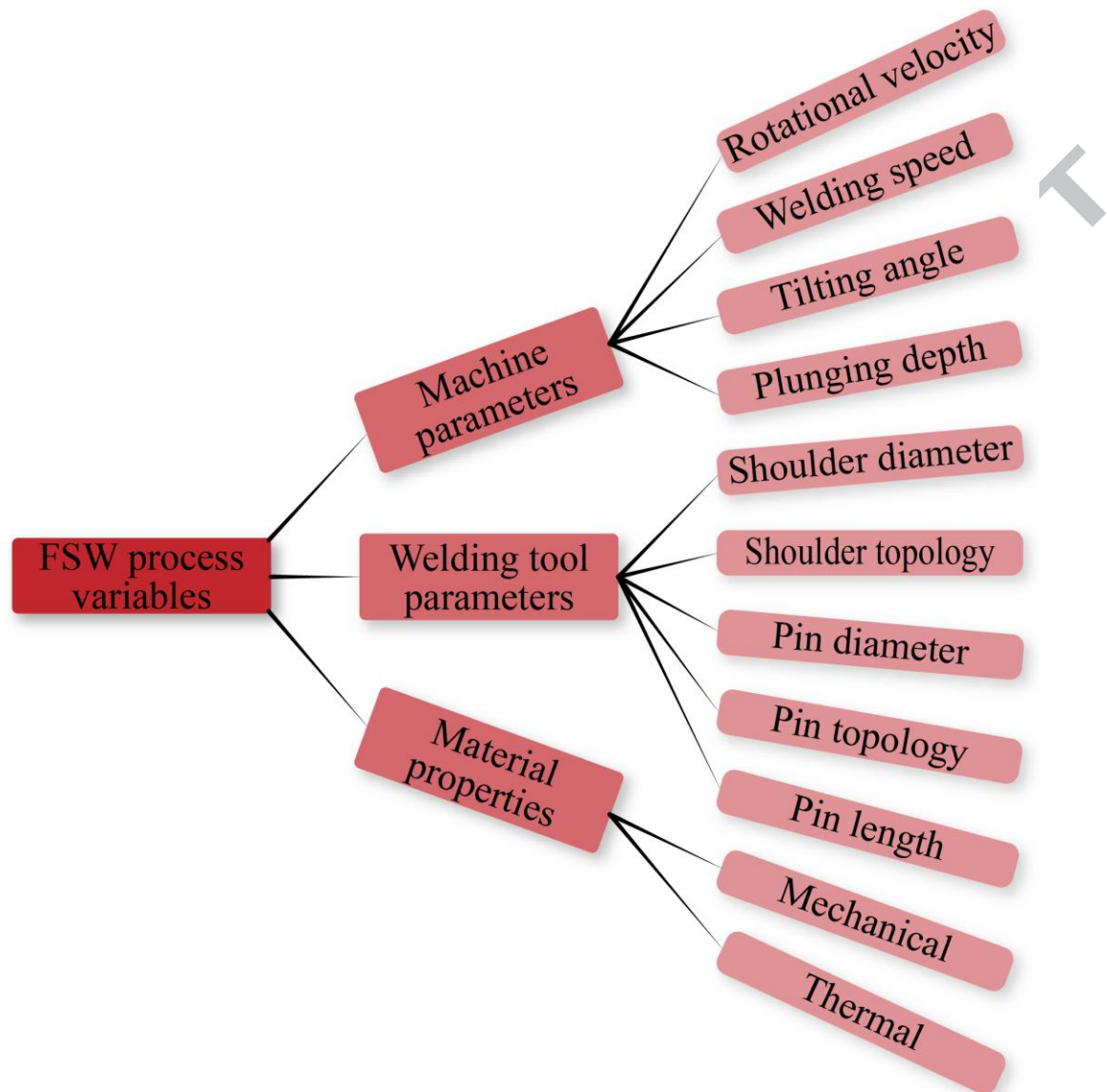
Table 5 Optimum combination of process parameters for stationary shoes FSW of polymer.

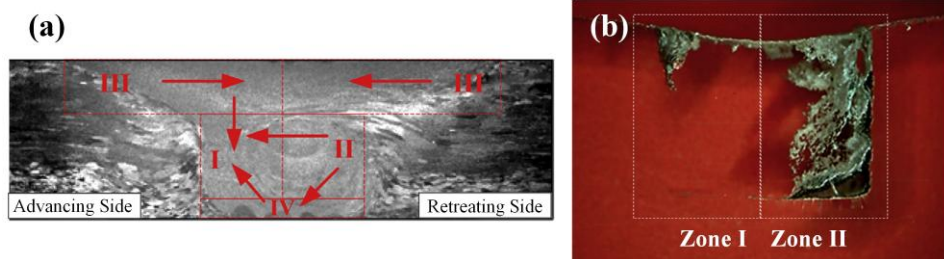
Table 6 Maximum shear-tensile strengths of various polymer-metal hybrid lap joints obtained by different techniques.

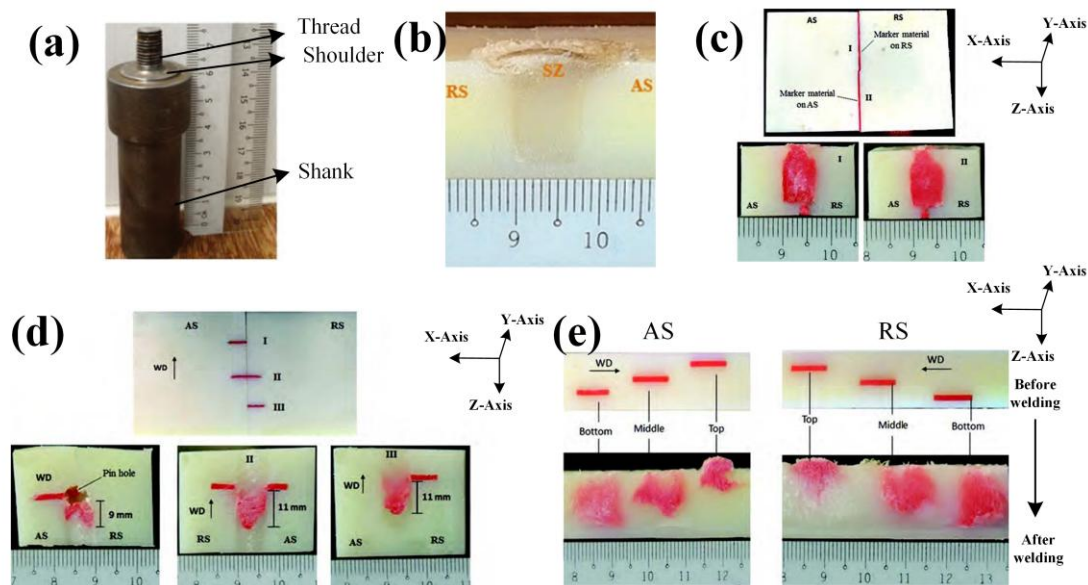
Table 7 Advantages, disadvantages and future research needs of different joining techniques accompanies with Table 6.

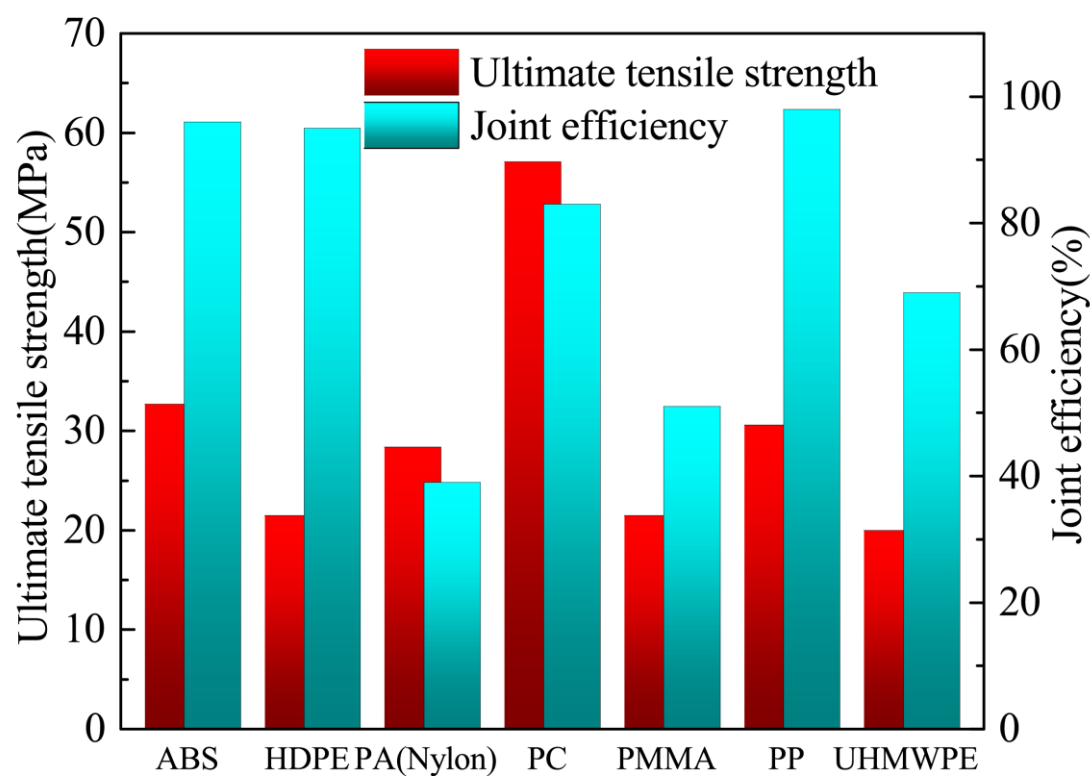


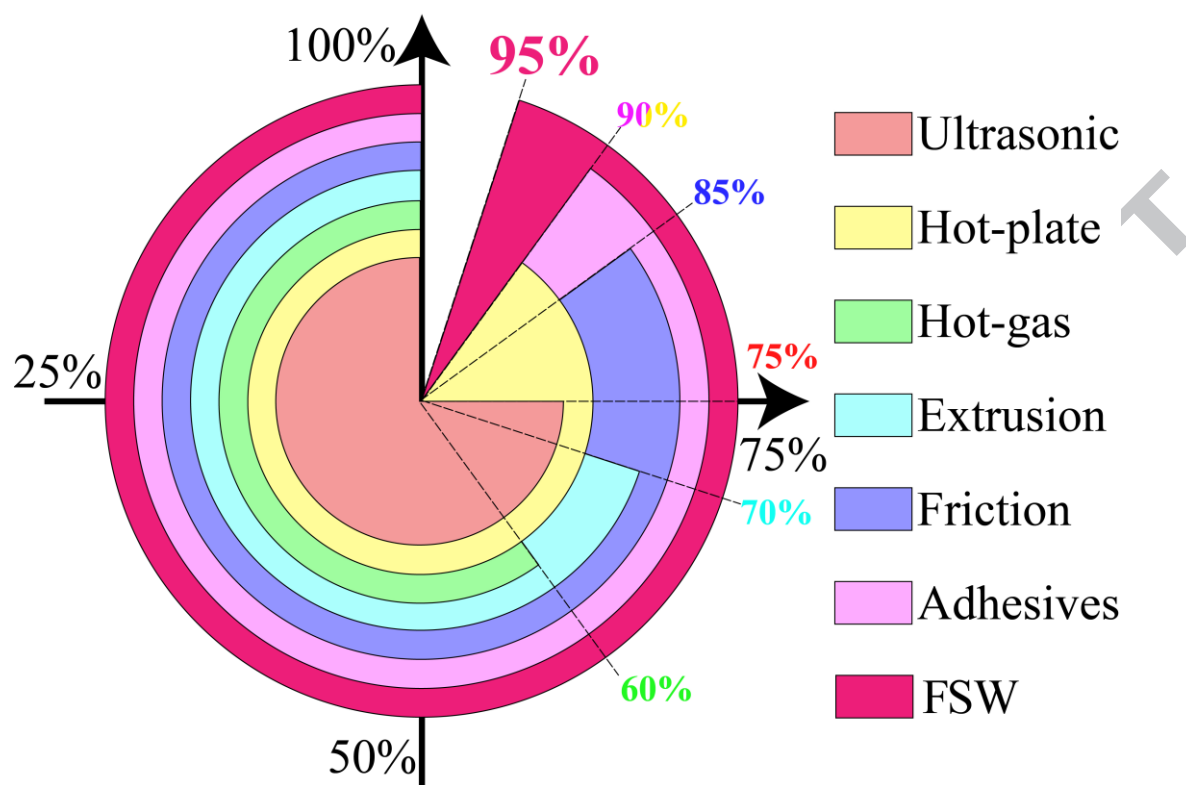


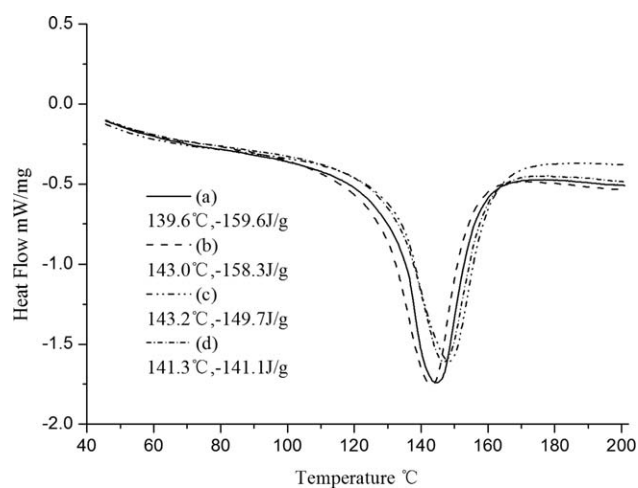




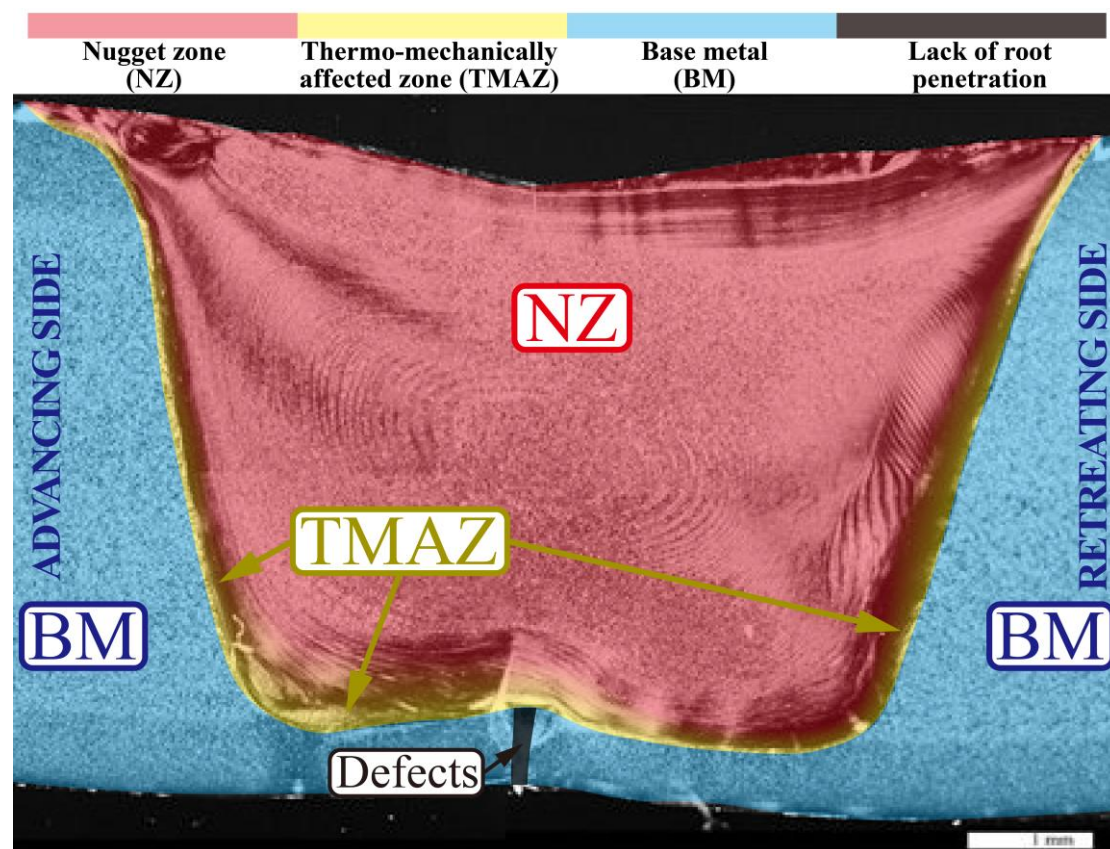


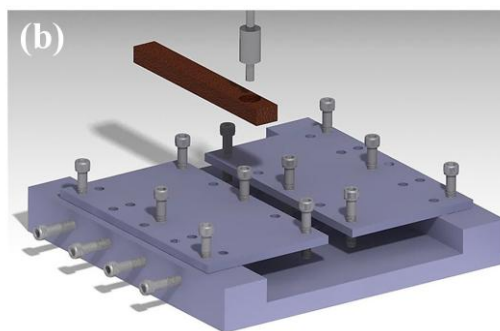
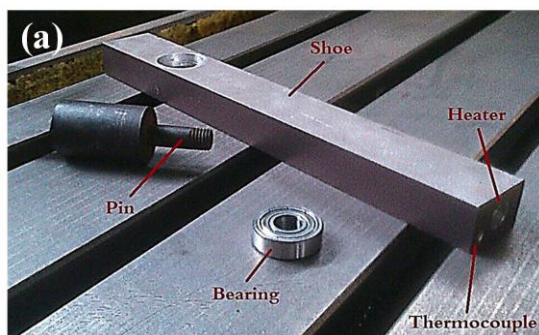


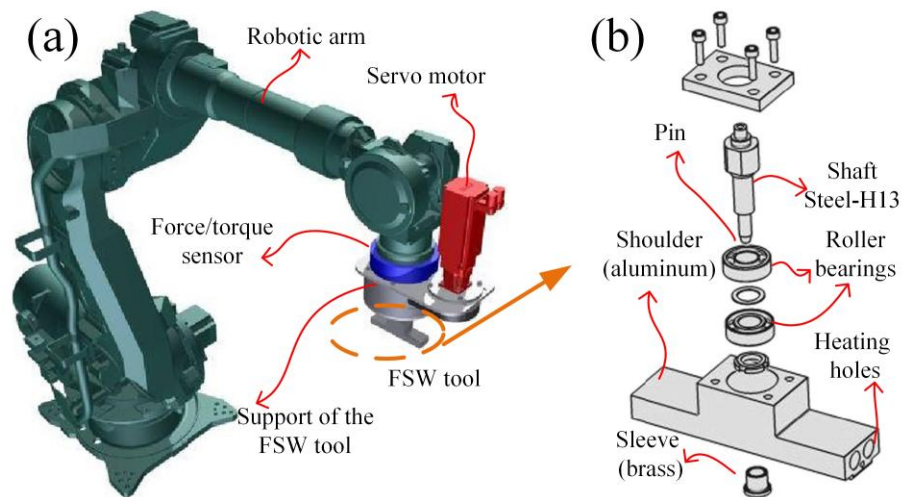


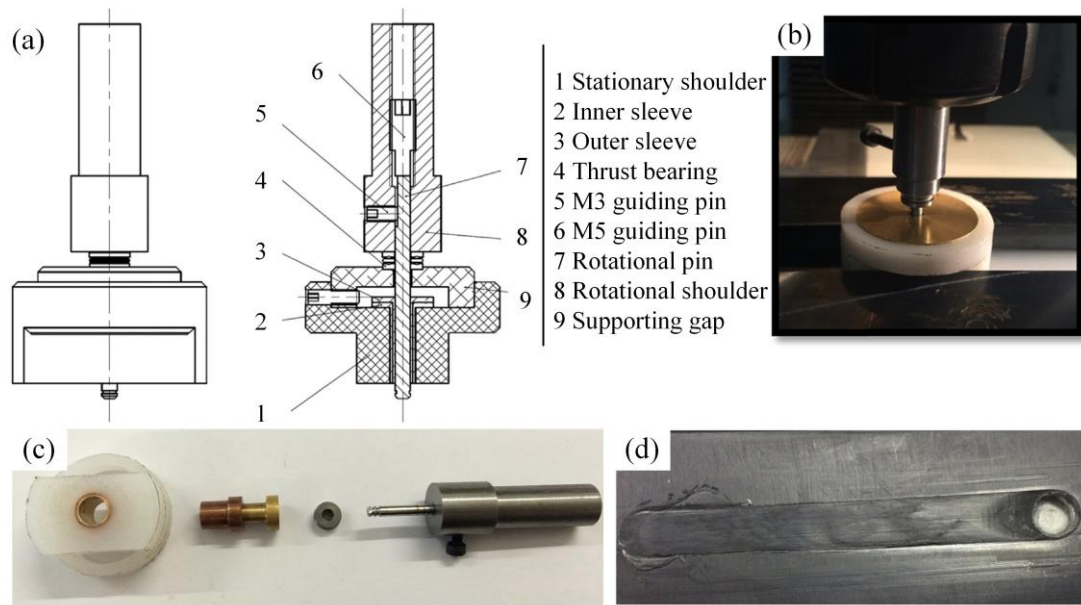


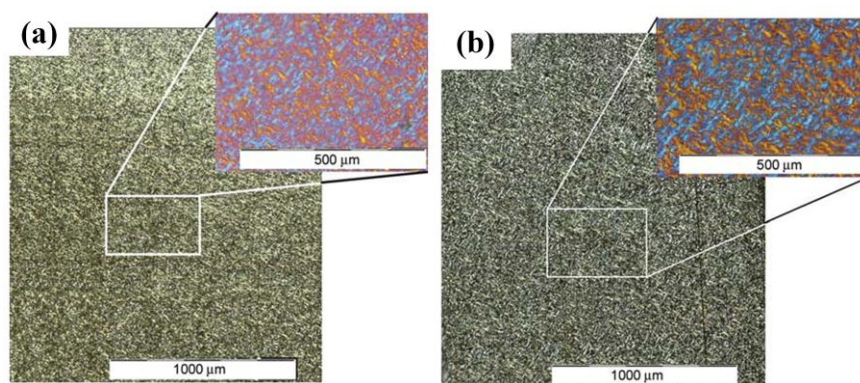


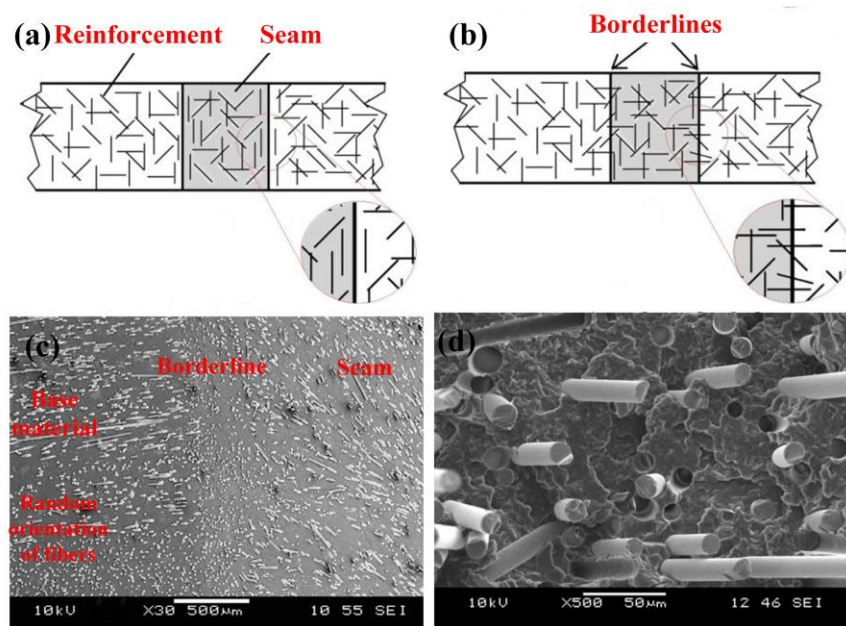


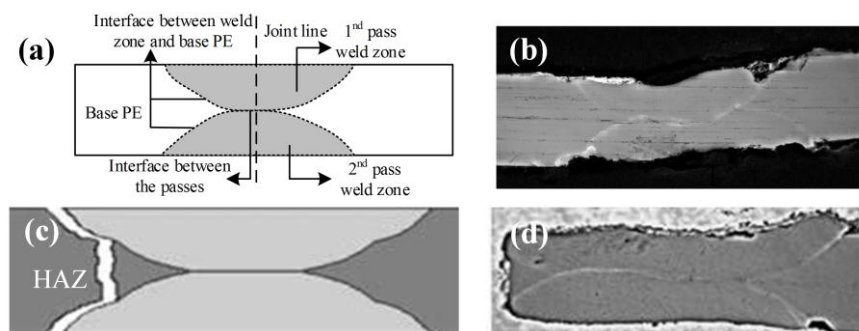




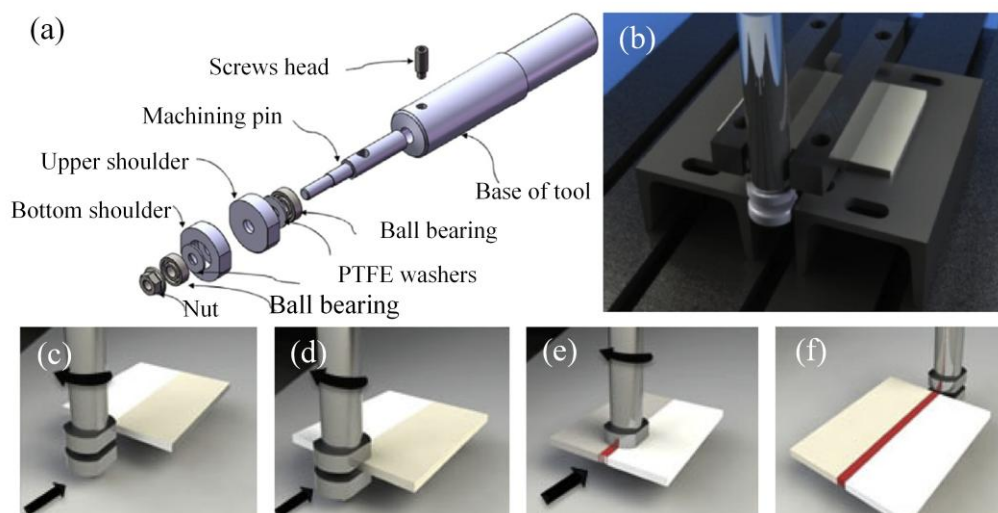


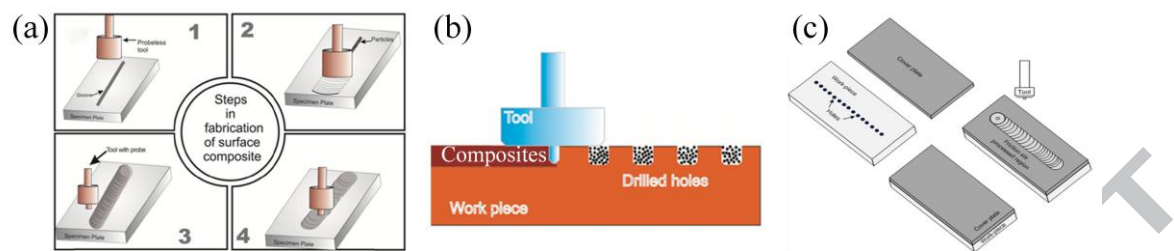


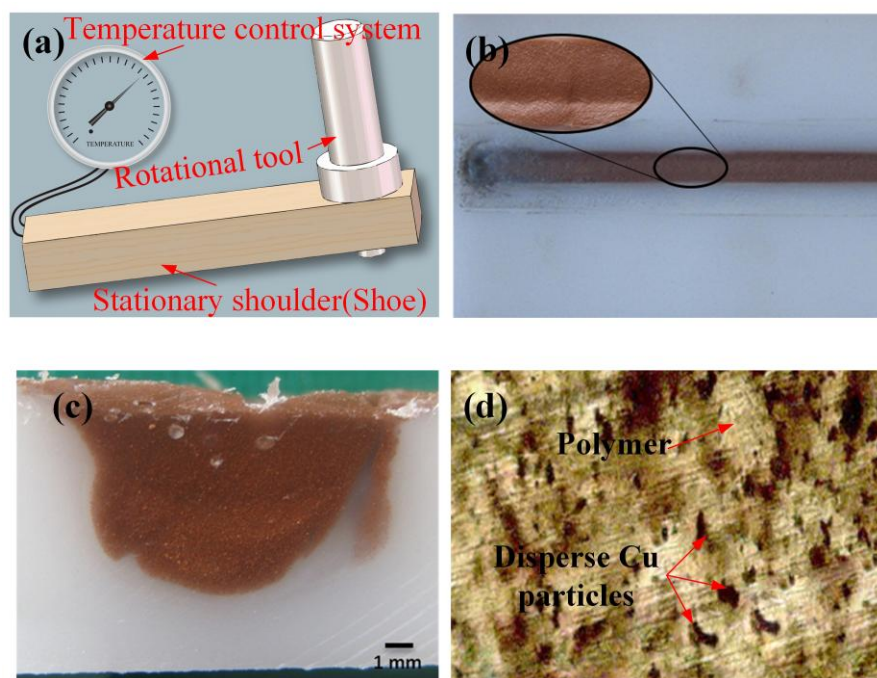


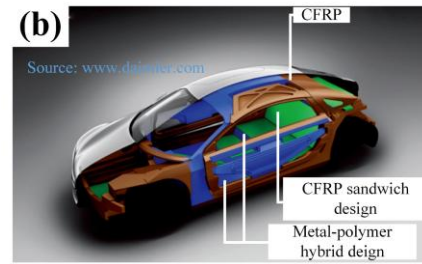
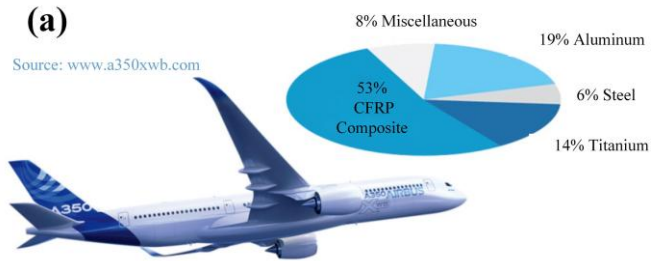


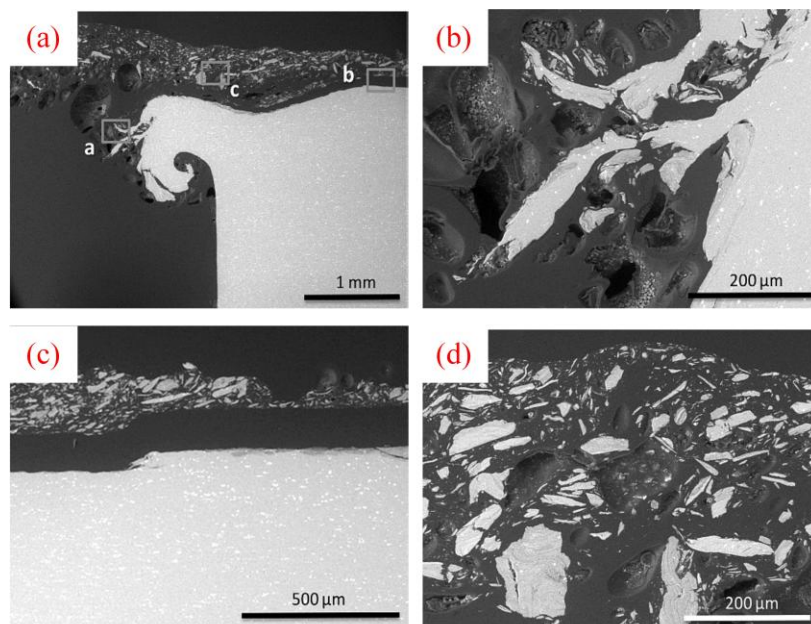












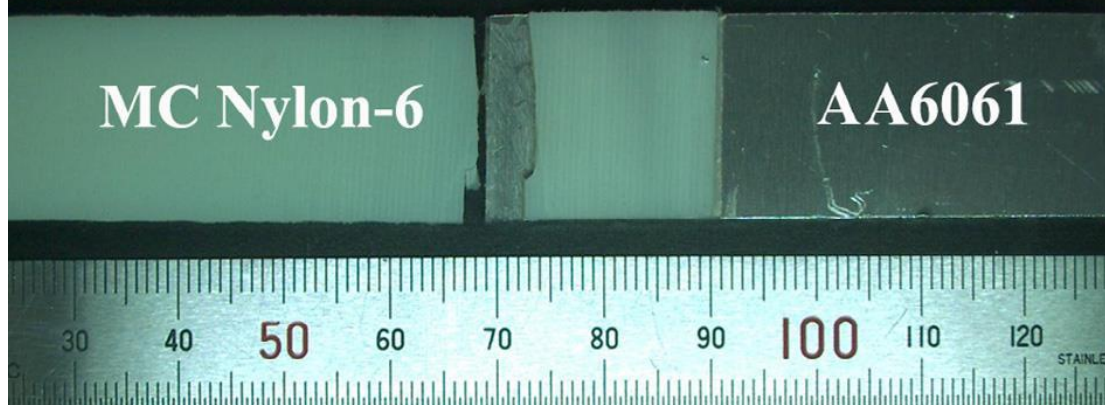
**(a) Front view of hybrid FLW joint**



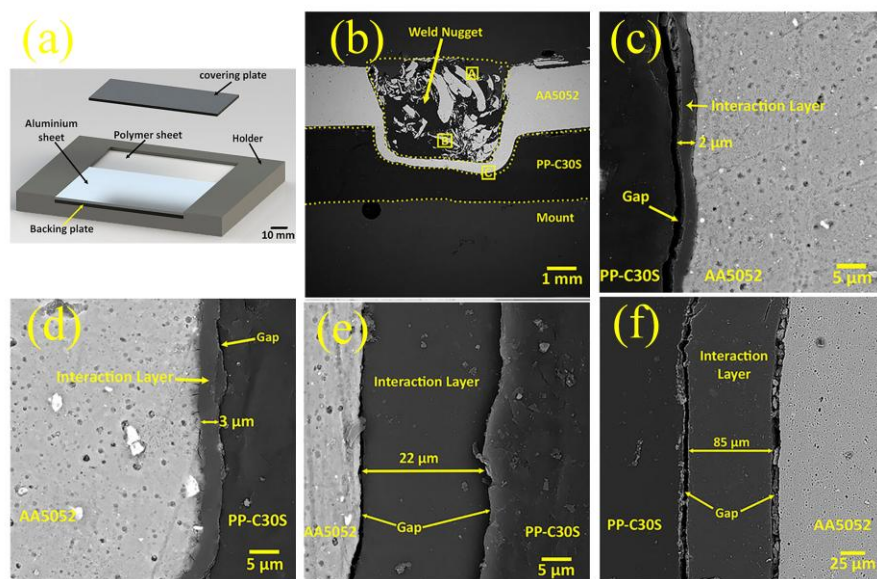
**(b) Back view of hybrid FLW joint**



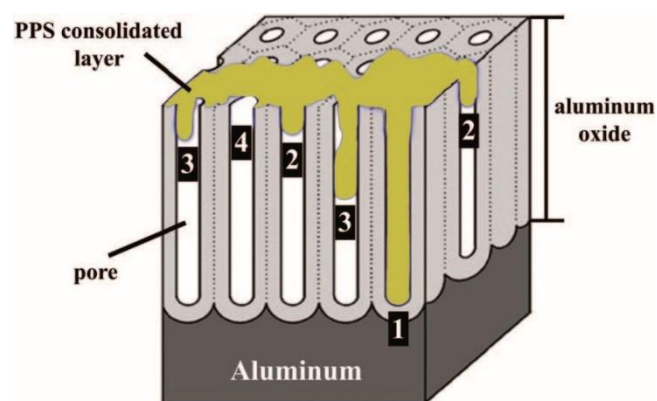
**(c) Back view of failed hybrid FLW joint**

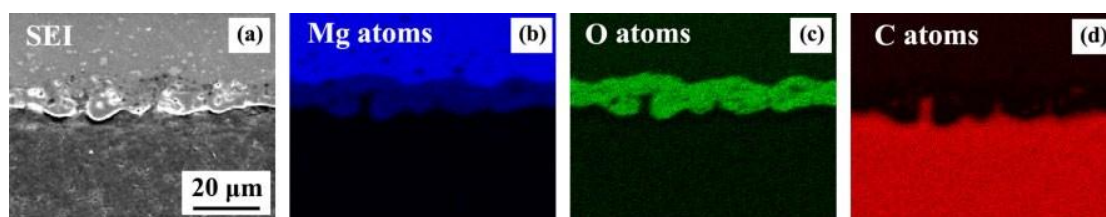


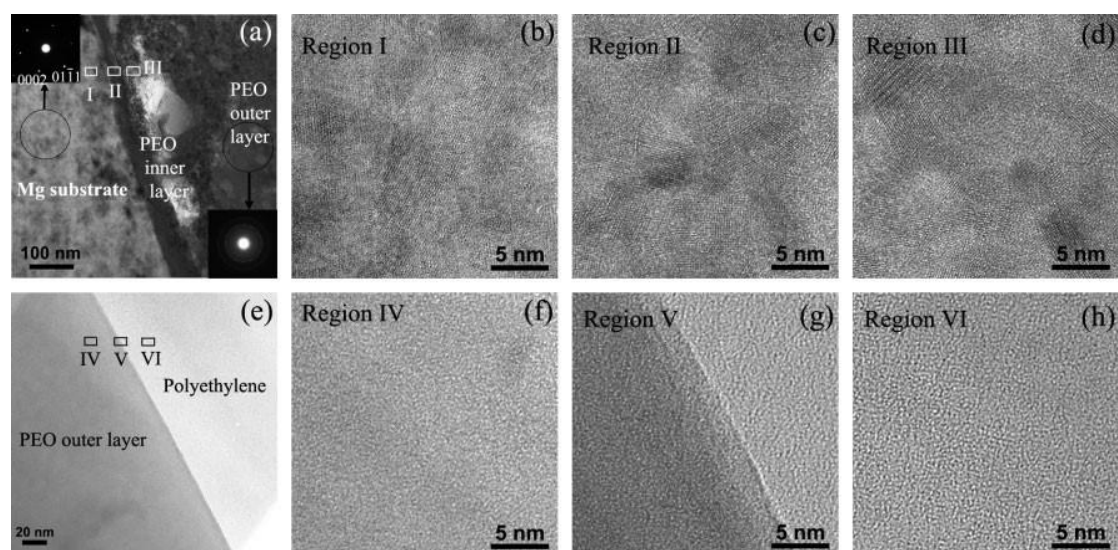


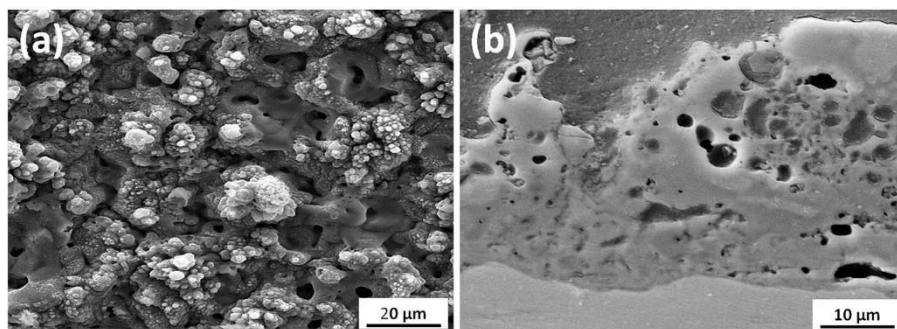


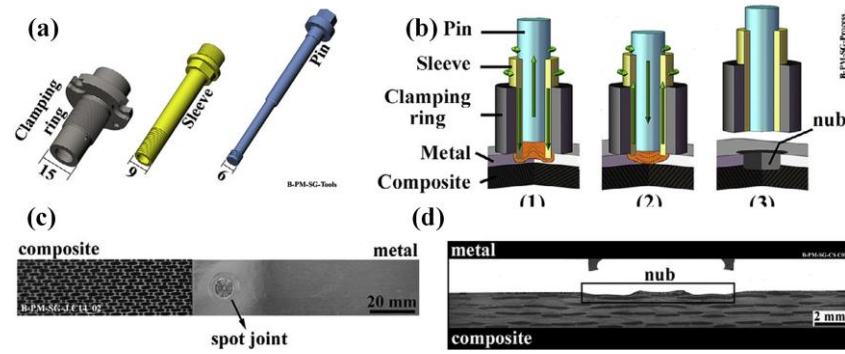


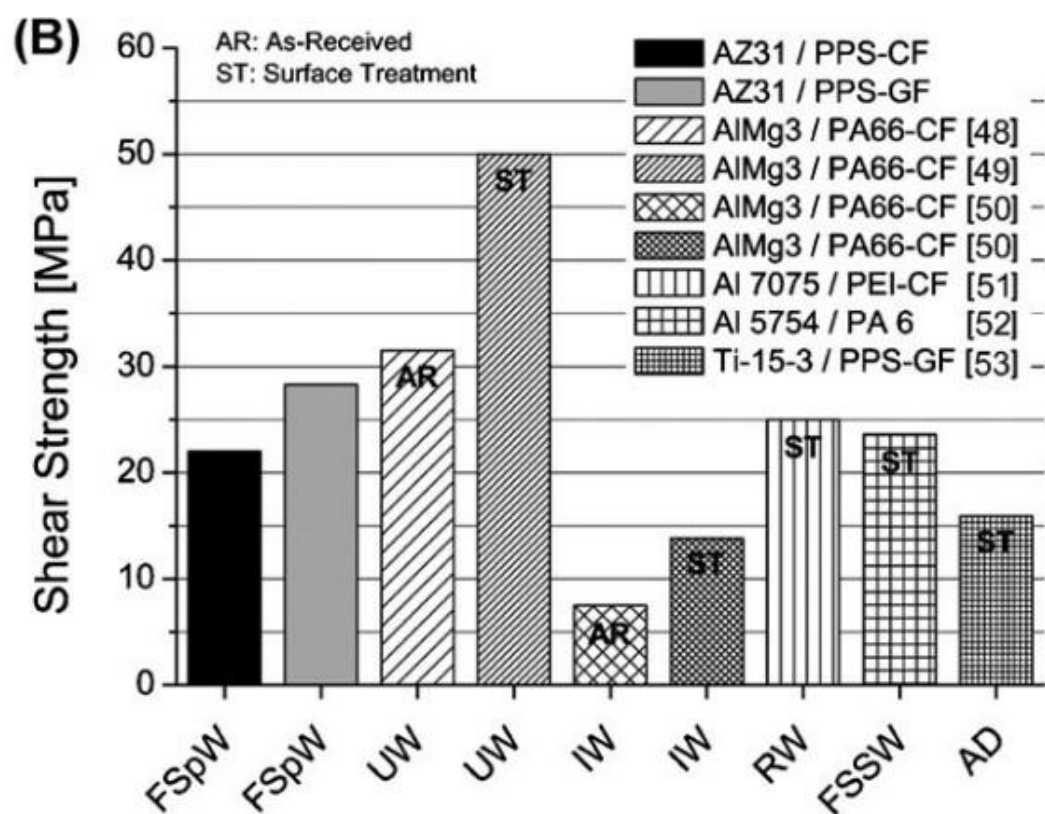












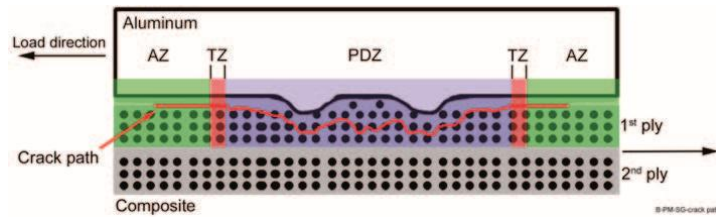


Table 7 Comparison of process requirements for polymer joining methods for 12 in. long butt weld in 0.25 in. thick PP [1].

Process	Preparation	Process time	Total time	Consumables	Machine/Tool consumable cost
Ultrasonic	energy directions	1-3 s	5-10 min	none	\$30,000
Hot-plate	none	30-40 s	60-90 s	none	\$47,000
Hot-gas	v-groove	8-10 min	15 min	gas, filler	\$3,500
Extrusion	v-groove	8-10 min	15 min	gas, filler	\$5,000
Friction	flatten face	10-15 s	6-8 min	none	\$89,000
FSW	none	2 min	3 min	none	\$11,000



ACCEPTED MANUSCRIPT

Table 8 Optimum combination of rotational velocity and welding speed for FSW of polymers.

Materials	Thickness (mm)	$\omega$ (rpm)	$v$ (mm/min)	Reference
PMMA	10	700	25	Simões et al. [13]
Nylon-6	10	1000	10	Zafar et al. [14]
PP 30% glass fiber	5	630	8	Payganeh et al. [16]
PP 20% carbon fiber	4	1250	25	Ahmadi et al. [17]
HDPE	4	3000	115	Bozkurt et al. [23]
PP	10	900	70	Sharma et al. [28]

Table 9 Welding tools used in the published papers during conventional FSW of polymer.

Shoulder		Pin		References
Diameter (mm)	Diameter (mm)	Topology	Length (mm)	
24	6	Thread	10	Panneerselvam et al. [33]
25	7.5	Thread	14	Zafar et al. [14]
15	5	Cylindrical	4.8	Jaiganesh et al. [26]
15	5 to 3	Taper	4.8	
15	5 to 2.5	Cylindrical grooved	4.6	
15	5 to 3	Taper pin with groove	4.8	
15	5	Triangle pin with screw thread	4.8	
15	5	Triangle pin	4.8	Payganeh et al. [16]
15	5	Cylindrical pin with groove	4.8	Hoseinlghab et al. [27]
15	7	Conical	7	
20	8	Conical	8	
				Sadeghian et al. [12]

Table 10 Typical defects appeared at the joint during FSW of polymer.

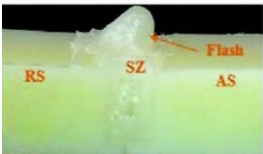
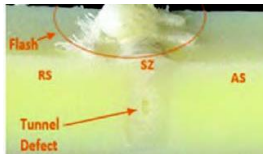
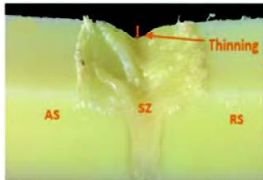
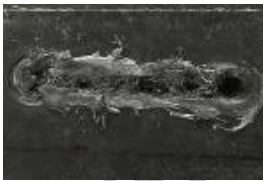
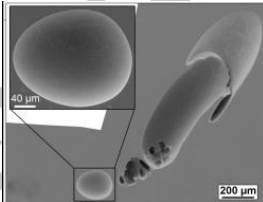

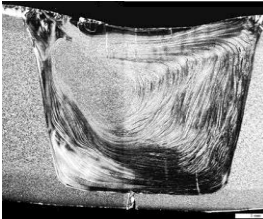
Defect	Typical defect	Definition	Possible causes
Flashes [14]		Excessive overflowing of materials on the top surface leaving a corrugated or ribbon like effect along the RS or AS.	Excessive forge load or plunge depth; Excessively hot weld; Smaller shoulder diameter
Tunnel [14]		Through inside cavity along the welding direction	Insufficient material flow; Improper welding tool; Overflowing of materials; Smaller plunge depth
Thickness reduction [14]		The thickness of NZ is lower than BM	Bigger plunge depth; Overflowing of materials; Improper backing support
Surface lack of filling [17]		A continuous dented surface characterized by insufficient fill with plasticized materials	Insufficient material flow; Improper backing support; Insufficient forge pressure; Overflowing of materials
Pore [41]		Hole featured by circle owing to the melting of materials	Excessively hot weld; Overflowing of plasticized materials; Insufficient forge pressure
Voids at the RS [13]		Lack of joining induced by insufficient consolidated and forged materials at the RS	Lower heat input; Excessive travel speed; Insufficient material flow; Improper welding tool
Lack of root penetration [1]		Lack of joining at the back area of butt plate	Shorter pin length; Smaller plunge depth; Bigger fitting gap or manufacturing errors

Table 11 Optimum combination of process parameters for stationary shoes FSW of polymer

Materials	Thickness (mm)	$T$ (°C)	$\omega$ (rpm)	$v$ (mm/min)	Joint efficiency (%)	References
HDPE	10	140	1600	25	95	Mostafapour et al. [43]
Nylon 6	6	150	630	20	98	Mostafapour et al. [4]
Wood/plastic	6	160	1600	8	93	Rahbarpour et al. [45]
PP/PC	1.5/2.6	0	1800	30	50	Eslami et al. [46]

PP/PE	8/8	0	1860	12.5	98	Hajideh et al. [47]
ABS	6	0	1500	100	60	Mendes et al.[25]
ABS	6	115	1500	96	76	Mendes et al. [24]
PP	7	160	1080	51	92	Strand et al. [1]
ABS	5	100	1600	20	89	Bagheri et al. [48]
PETG	10	0	1200	50	90	Kiss et al. [15]

Table 12 Maximum shear-tensile strengths of various polymer-metal hybrid lap joints obtained by different techniques

Process	Max. strength (% of polymer strength)	Calculation method of strength	Reference
FLW	7.8 MPa (10.3%)	Max. Load/(Sample width × Length of lapped area)	Liu et al. [79]
FSW	4.72 MPa (15.1%)	Max. Load/(Sample width × Effective joining thickness)	Rahmat et al. [80, 81]
FLW	12.9 MPa (9.2%)	Max. Load/(Sample width × Shoulder diameter)	Nagatsuka et al. [76]
FLW	5.75 MPa (9.3%)	Max. Load/(Sample width × Pin diameter)	Ratanathavorn et al. [82]
FLW	5.1 MPa (16.3%)	Max. Load/(Sample width × Shoulder diameter)	Shahmiri et al. [83]
Adhesive bonding	3.1~13.3 MPa (5~22%)	Load at failure/Bonded area	Boone et al. [77]

Table 7 Advantages, disadvantages and future research needs of different joining techniques accompanies with Table 6.

Process	Advantages	Disadvantages	Future research needs
FSW	Butt joint; mechanical interlocking; teeny degradation; short joining time	Complex pin topology design; high axis force; narrow molten region	Optimizing pin topology and welding parameters
FLW	Lap joint; high quality; teeny degradation of polymer; simple shoulder design	Bubbles; no mechanical interlocking; gap induced by difference of thermal expansion coefficient	Groping optimal surface pre-treatment; reducing bubbles and degradation
FSLW	Lap joint; mechanical interlocking; teeny degradation; thicker sheet	Complex pin topology design; surface pre-treatment; complex parameter variables	Optimizing pin topology and welding parameters; surface pre-treatment
Adhesive bonding	Big joining area; good sealing of joint; avoiding galvanic corrosion; less stress concentration	Complex surface contamination removal and pre-treatment; bad impact resistance; long process cycle	Improving impact resistance; increasing mechanical interlocking